



**Catalytic C–H bond functionalisation chemistry: the case for  
quasi-heterogeneous catalysis**

Journal:	<i>ChemComm</i>
Manuscript ID	CC-FEA-08-2015-006980.R1
Article Type:	Feature Article
Date Submitted by the Author:	17-Sep-2015
Complete List of Authors:	Reay, Alan; University of York, Chemistry Fairlamb, Ian J. S.; University of York, UK, Chemistry

## Catalytic C–H bond functionalisation chemistry: the case for quasi-heterogeneous catalysis

 Alan J. Reay<sup>a</sup> and Ian J. S. Fairlamb<sup>a,\*</sup>

 Received 00th January 20xx,  
Accepted 00th January 20xx

DOI: 10.1039/x0xx00000x

www.rsc.org/

This feature article examines the potential of heterogeneous Pd species to mediate catalytic C–H bond functionalisation processes employing suitable substrates (*e.g.* aromatic/heteroaromatic compounds). A focus is placed on the reactivity of supported and non-supported Pd nanoparticle (PdNPs) catalysts, in addition to the re-appropriation of well-established heterogeneous Pd catalysts such as Pd/C. Where possible, reasonable comparisons are made between PdNPs and traditional ‘homogeneous’ Pd precatalyst sources (which form PdNPs). The involvement of higher order Pd species in traditional cross-coupling processes, such as Mizoroki–Heck, Sonogashira and Suzuki–Miyaura reactions, allows the exemplification of potential future topics for study in the area of catalytic C–H bond functionalisation processes.

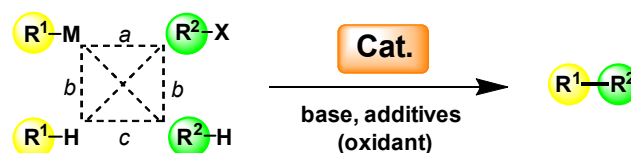
### Introduction

Great effort has been directed towards the selective and catalytic functionalisation of C–H bonds.<sup>1, 2</sup> These processes are usually mediated by a transition metal for which the reaction mechanisms are often intriguing and where the products formed are useful in many areas of scientific research and endeavour.

Removing substrate pre-functionalisation usually minimises downstream chemical waste, while eliminating the need for prior mandatory reaction steps for the installation of chemical functionality which is ultimately lost in the final and desired chemical transformation. One can compare three complementary reactions (**Scheme 1**): (a) a traditional cross-coupling reaction of an organohalide with an organometallic reagent; (b) the direct reaction of an organohalide or organometallic with a substrate containing a reactive C–H bond (note: a base is needed for the former and an oxidant for the latter); (c) the selective reaction of two substrates containing C–H bonds (by an oxidative dehydrogenative process). There is thus a strong case for developing synthetic methods that facilitate the selective C–H bond functionalisation of any desired molecule. Couplings at C–H bonds can be made involving sp, sp<sup>2</sup> and sp<sup>3</sup> centres, although the latter might be viewed as challenging.

In terms of elemental sustainability it is important that effort is directed towards unlocking the potential of cheaper, less toxic and more abundant metals as catalysts. In doing so it is essential to examine the overall waste associated with a given chemical transformation. It is also imperative that current elemental usage levels, as well as issues regarding the

criticality of supply chains, are examined before making the assertion that a cheaper and more abundant element today will be more readily available than a precious element in, for example, 60 years.<sup>3</sup>



**Scheme 1.** A generic scheme to represent traditional cross-coupling and C–H bond functionalisation processes (in this example, R<sup>1</sup> and R<sup>2</sup> are carbon-centred, M = metal and X = halide or pseudohalide, *i.e.* leaving group).

Given the breakthroughs made in the field of catalytic Pd-catalysed cross-coupling chemistry, it is not unreasonable to ask whether research should shift focus to other, more elementally sustainable first-row transition metals such as Mn,<sup>4, 5</sup> Fe<sup>6, 7</sup> or Co.<sup>8–10</sup> While that is of global importance, it is of equal value to determine whether Pd catalysts can be better utilised and recycled,<sup>11–14</sup> so that future generations can exploit and benefit from the remarkable reactivity of this precious metal. Furthermore, one can question whether the reaction mechanisms involving Pd are fully understood, especially those reactions involving the catalytic functionalisation of C–H bonds. To date the mechanistic picture is dominated by homogeneous catalytic cycles involving one or two Pd atoms, involving Pd<sup>0</sup>, Pd<sup>II</sup>, Pd<sup>III</sup> and Pd<sup>IV</sup> oxidation states.<sup>15–31</sup> Moreover, researchers are often quick to rule out or entirely ignore a role for heterogeneous species in catalysis, either directly (*i.e.* by substrate activation) or indirectly (*i.e.* acting as a Pd reservoir, regulating the Pd concentration).

Central to the topic of this paper is to recognise that precious metal catalysts such as Pd can play a critical role in the C–H bond functionalisation of organic molecules, where

<sup>a</sup> Department of Chemistry, University of York, Heslington, York, YO10 5DD, UK.

\* Email: ian.fairlamb@york.ac.uk. Tel: 0044 (0)1904 324091.

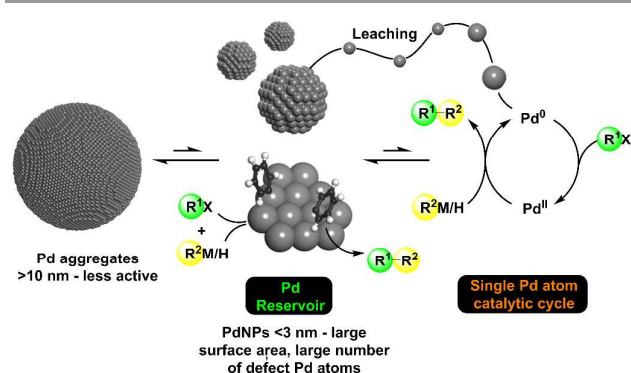
DOI: 10.1039/x0xx00000x

current and new methodologies can be exploited for years to come. A focus is placed on understanding that common Pd precursor catalysts (precatalysts) are able to aggregate to form higher order Pd species (*i.e.* usually nanoparticles), which can become catalytically relevant under an eclectic array of reaction conditions. Established processes and findings from the field of traditional cross-coupling chemistry are described to provide prior context, particularly: (1) the use of well-defined and supported Pd nanoparticles (PdNPs) as catalysts; (2) the evolution, propagation and catalytic role of PdNPs formed *in situ* from common Pd precatalysts. Examples from C–H bond functionalisation reactions studied in our laboratories are showcased, while recent developments in the use of heterogeneous Pd catalysts from a number of sources, including well-defined PdNPs in catalytic C–H bond functionalisation reactions, are discussed in detail. A perspective on the future of this topical area of research is offered at the end of this article.

## A brief overview of the role played by Pd nanoparticles in Mizoroki–Heck, Sonogashira and Suzuki–Miyaura cross-coupling reactions

### Background

Historically, concerning the nature of the active Pd catalyst species in Mizoroki–Heck cross-coupling reactions, there has been significant debate about the involvement of homogeneous and heterogeneous Pd species. There is unequivocal evidence showing that homogeneous Pd precatalyst sources (*e.g.* Pd(OAc)<sub>2</sub>) can aggregate to form higher order species such as PdNPs – spherical PdNPs are typically 2–4 nm in size, with substantially different surface areas. The key question for cross-coupling chemistry concerns the catalytic role of PdNPs. Are the aggregated Pd species simply a dead-end for catalysis, *i.e.* an inactive form, or can they act as a Pd reservoir, controlling the active Pd within the catalytic cycle, or are they directly participating in surface catalysis? It is possible to represent this phenomenon as shown in Scheme 2.



**Scheme 2.** A schematic representation showing a role for aggregated Pd (Pd reservoir) with leached single Pd atoms.

It is important to recognise that most studies point to single Pd atoms leaching from the surface of PdNPs. By way of an example, a 2 nm PdNP consists of about 250 Pd atoms, thus if the PdNPs are spherical *i.e.* truncated icosahedra with (111) planes, then about one fifth of these Pd atoms are available for a reaction on the surface. The equilibrium position between Pd reservoir and leached Pd is therefore critical to catalytic activity and efficacy.<sup>32</sup> Many articles and key reviews have grappled with this subject over the years.<sup>33–36</sup> It is not the intention of this article to more broadly discuss these issues, but simply to provide a context to better understand the potential role that higher order Pd species can play in catalytic C–H bond functionalisation chemistry. It is however clear, a multi-ensemble of higher order Pd species play a key role in traditional catalytic cross-coupling processes, meaning that several catalytic cycles can be operative in solution. The mechanistic picture is nicely illustrated by comparing a simple road roundabout, *i.e.* a catalytic cycle involving a single species, with the multiple ‘magic roundabout’ found in Swindon in the United Kingdom, the analogy being that several catalytic species operate in similar cycles which contribute to an overall catalytic process.



**Figure 1.** Top: a normal roundabout exemplifying a single catalytic cycle; Bottom: the reality of Pd-catalyzed cross-coupling chemistry (in the absence of strongly coordinated and well-defined ligands) and their multiple catalytic cycles, here exemplified by the ‘magic roundabout’ in Swindon, UK (signs sourced from Google, under creative commons search).

### The evidence from Mizoroki–Heck and Sonogashira cross-coupling reactions

Central to the topic of this article is recognition of the existence of a Pd reservoir in catalytic cross-coupling processes. Workers at DSM Pharma Chemicals discovered that the Mizoroki–Heck cross-coupling of bromobenzene with *n*-butyl acrylate mediated by Pd(OAc)<sub>2</sub> exhibited an inverse

relationship (negative order in Pd) of catalytic activity with catalyst concentration (Figure 2).<sup>37</sup>

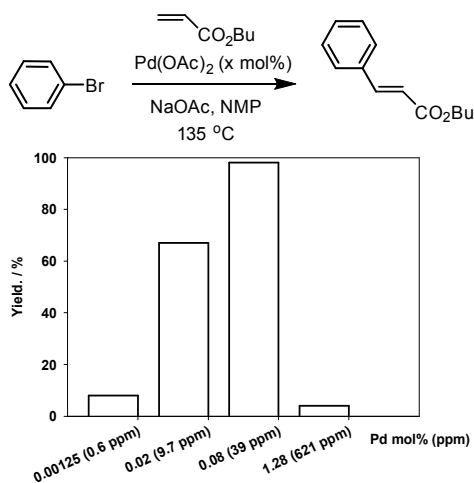


**Figure 2.** Inverse relationship between catalytic activity and concentration in a Mizoroki-Heck cross-coupling (de Vries *et al.*, 2003).<sup>37</sup> Adapted with permission from *Org. Lett.*, 2003, 5, 3285.

The Pd catalyst loading which gave the highest yield was found to be 0.08 mol% (39 ppm; calculated from the experimental data reported in the original paper). Moving to either lower or higher Pd catalyst loadings resulted in a loss of catalyst activity. This observation can be attributed to the aggregation of Pd at higher Pd concentrations, which can be associated with the precipitation of Pd black (often seen at the end of cross-coupling reactions when the substrate is exhausted). At this concentration of Pd it is not entirely obvious what the structure of the Pd catalyst is. ESI-MS studies (–ve mode) provided some insight, showing the presence of PdBr<sub>3</sub><sup>–</sup> under working reaction conditions. This phenomenon was also noted in the Sonogashira cross-coupling of 4-bromoacetophenone with phenylacetylene using palladacyclic precatalysts in work conducted by our group (Figure 3).<sup>38</sup> In this case, optimal turnover frequencies (TOFs) were recorded at 0.01 mol% Pd (92 ppm Pd). It is notable that in mechanistically distinct cross-coupling reactions with differing reaction conditions (*i.e.* catalyst structure, solvent type and additives), these reactions are most active when the concentration of Pd is below 100 ppm. We can confidently predict that this is the case for the majority of cross-coupling processes utilising activated organohalide substrates, where transmetalation and reductive elimination are not seen as problematic, *e.g.* side reactions such as homocoupling and hydrodehalogenation/protodemetalation are not seen.

It is worthy of note that Leadbeater and co-workers determined that Pd concentrations as low as *ca.* 20–50 ppb were able to effect certain cross-coupling reactions under microwave conditions in water.<sup>39</sup> Again, these types of reaction typically employ activated substrates (aryl halides), for example reaction of 4-bromoacetophenone with phenylboronic acid in the presence of Pd(OAc)<sub>2</sub> (100 ppb) using K<sub>2</sub>CO<sub>3</sub> afforded the cross-coupled product in good yield.

These research findings serve to show that: (1) low Pd concentrations can be used for certain cross-coupling processes involving activated substrates (thus are also a poor test for catalyst screening); (2) that aggregated Pd species can ultimately cause a drop-off in catalyst efficacy at higher concentrations, leading to non-linear rate relationships with respect to Pd concentration.<sup>40</sup>

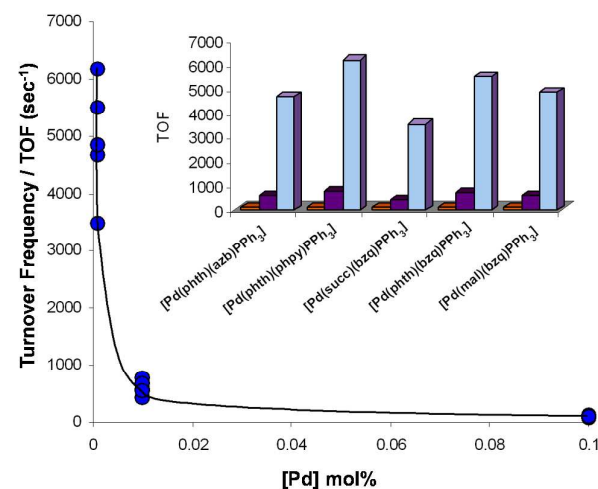
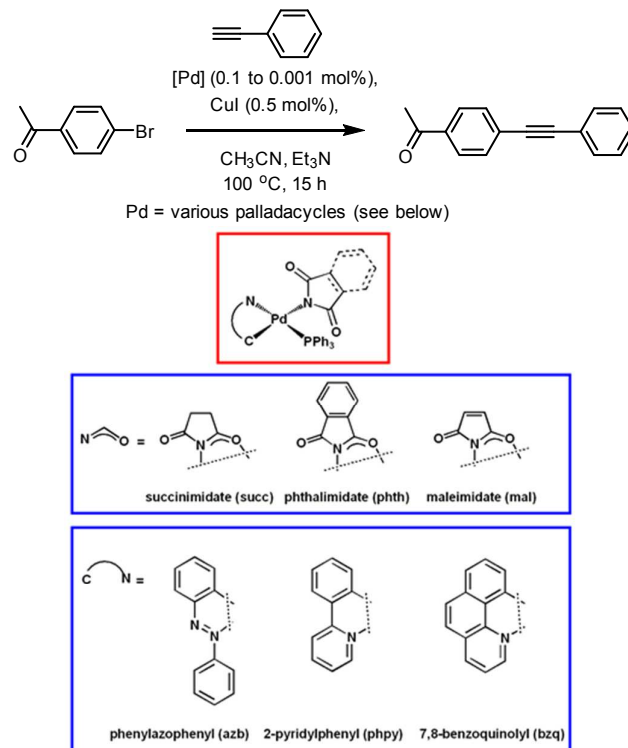


**Figure 3.** Effect of Pd catalyst loading in the Sonogashira cross-coupling of an activated aryl halide with a terminal alkyne (Fairlamb *et al.*, 2004).<sup>38</sup>

For Mizoroki-Heck cross-couplings the role of the Pd reservoir has been investigated by several research groups, in order to determine whether this reservoir simply releases single atoms into a homogeneous catalytic cycle, or whether the activation

of aryl halides occurs directly at Pd surfaces. Evidence for the leaching of catalytically active Pd has been reported from supported Pd catalysts (e.g. Pd/C, Pd/SiO<sub>2</sub>, Pd/γ-Al<sub>2</sub>O<sub>3</sub>).<sup>41, 42</sup> The release of Pd is concomitant with recapture of Pd at the surface. The mechanism of leaching has been studied by Dupont and co-workers, who showed that oxidised Pd<sup>II</sup> species were released into solution from higher order aggregated Pd species stabilised by quaternary ammonium salts.<sup>43</sup>

Further support for the leaching of Pd from larger PdNPs (~15 nm) has been observed in work by Rothenberg and co-workers.<sup>44</sup> Using a reactor containing a membrane which was able to select for particles <5 nm it was demonstrated that sintering of the PdNPs occurred under Mizoroki–Heck cross-coupling conditions (note: PdNPs of less than 5 nm can in theory contain several thousand Pd atoms). In keeping with the work described above, Rothenberg also characterised 'Pd<sup>II</sup>-(X)Ar(L)*n*' species under working reaction conditions. The same group also followed the formation and subsequent growth of Pd clusters from several Pd<sup>II</sup> precursors using UV–visible spectroscopy, allowing for modelling of the reduction, cluster growth and aggregation of such species.<sup>45</sup>

X-ray absorption spectroscopic (XAS) analysis by Baiker and co-workers led them to conclude that Pd atom leaching occurs under working reaction conditions. Quick scanning extended X-ray absorption fine structure (QEXAFS) measurements allowed the characterization of PdNPs leached from a solid Pd catalyst (Pd on an Al<sub>2</sub>O<sub>3</sub> support) to be monitored in real time on a sub-second timescale.<sup>46</sup> This technique, requiring synchrotron radiation, allows the local structure of ordered materials such as PdNPs to be characterised, in addition to molecular species like PdBr<sub>4</sub><sup>2-</sup> and Pd<sub>2</sub>Br<sub>6</sub><sup>2-</sup> anions. The Mizoroki–Heck reaction of bromobenzene and styrene mediated by Pd/Al<sub>2</sub>O<sub>3</sub> only leached Pd at reaction temperatures of 150 °C. Crucially, the species released at this temperature were found to be PdNPs ca. 2 nm (i.e. during substrate turnover). Interestingly, when the reaction rate started to decrease, pronounced changes in the EXAFS spectra were noted, leading to the characterisation of evolving PdBr<sub>4</sub><sup>2-</sup> and Pd<sub>2</sub>Br<sub>6</sub><sup>2-</sup> anions. Such species appear to be present towards the latter stages of reaction when the concentration of bromobenzene is low and the concentration of Br<sup>-</sup> high. The authors concluded that the leached PdNPs can act beyond a simple Pd reservoir and are themselves catalytically active species, in addition to providing single-atom Pd species which are capable of entering into a traditional homogenous catalytic cycle.

#### Studies on Suzuki–Miyaura cross-coupling reactions

Working in collaboration with Lee, our group was able to test the catalytic competence of well-defined, polymer-supported PdNPs in a Suzuki–Miyaura cross-coupling reaction of phenylboronic acid and iodoanisole in methanol.<sup>47, 48</sup> The (poly)vinylypyrrolidone (PVP) polymer used is known to support and stabilise PdNPs, preventing agglomeration.<sup>49, 50</sup> A colloidal seeding method could therefore be employed to allow preparation of four different sizes of PVP–PdNPs, with mean diameters between 1.8 and 4.0 nm, which could be stored and

manipulated easily under air. Upon comparison of the activity of these catalysts as a function of TOF against the total number of surface Pd atoms, a clear trend was observed, with smaller particles displaying greater activity. If however the TOF was normalised against only those Pd atoms contained within defect sites on the truncated cuboctahedral particles, no difference between particle sizes was observed (Figure 4). This observation makes clear that it is the abundance of surface defect sites which determines the reactivity of such particles in this reaction; simply put, the more defect sites per particle, the more active the catalyst.

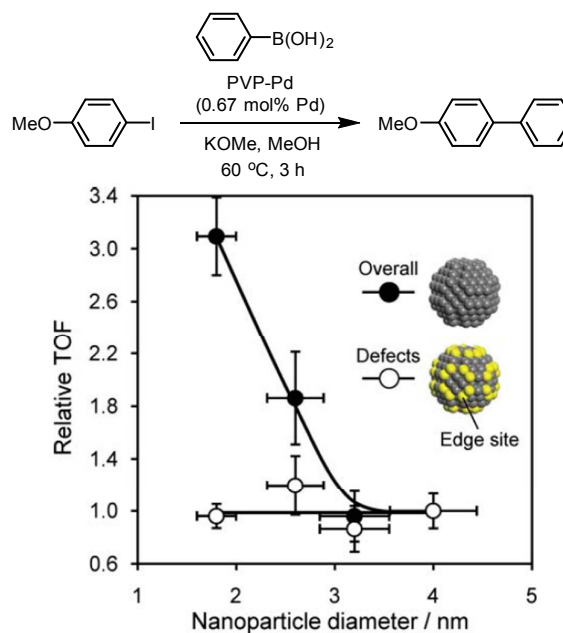


**Figure 4.** Relationship between TOF and particle size normalised to either total surface Pd atoms (●) or defect surface Pd atoms (○) in a Suzuki–Miyaura coupling of phenylboronic acid and iodoanisole (Fairlamb *et al.*, 2010).<sup>47, 48</sup> Reproduced from Ref 48 with permission from The Royal Society of Chemistry.

It is possible however that this trend was observed due to a preferential solubility of low-coordinate Pd species, leading to a more homogeneous catalytic manifold. To probe this effect further *in operando* X-ray absorption spectroscopy (XAS) was used to effectively monitor the coordination environment of the PdNPs, allowing for detailed analysis of the heterogeneity of the reaction under normal working conditions. These measurements indicated no sintering or leaching of the catalytically relevant particles during the reaction under the conditions used (Figure 5), a result confirmed by EXAFS, X-ray photoelectron spectroscopy (XPS) and transmission electron microscopy (TEM) studies. Importantly no induction period was seen, which is consistent with the observation that nanoparticulate Pd is not simply acting as a pre-catalyst or Pd reservoir (*vide supra*) – [Pd] responded in a first manner (contrast Pd(OAc)<sub>2</sub> which exhibits a negative order under the same reaction conditions). Finally, poisoning tests using elemental mercury (detailed below), performed during active substrate turnover, caused immediate cessation of catalytic

activity; the resultant Pd core/Hg shell particles were successfully characterised by XPS and a 1:1 correlation between the surface Pd and Hg atoms was observed.

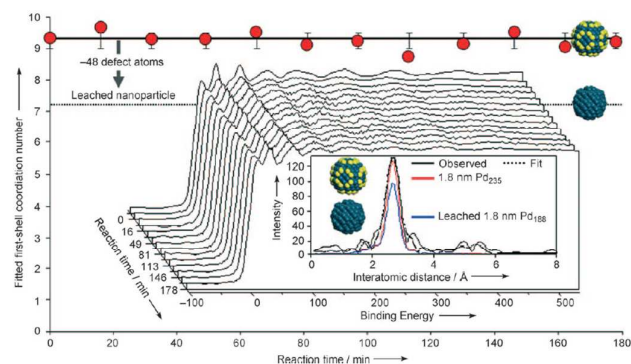


**Figure 5.** XAS spectra of a Suzuki–Miyaura cross-coupling indicating no change in PdNP coordination environment during active substrate turnover (Fairlamb *et al.*, 2010).<sup>47, 48</sup> Reproduced with permission from *Angew. Chem. Int. Ed.*, 2010, 49, 1820. Copyright 2010 WILEY-VCH Verlag GmbH & Co.

Subsequent work by McGlacken and co-workers probed the shape sensitivity of a Suzuki–Miyaura coupling of phenylboronic acid and bromoanisole, catalysed by palladium nanocubes (PdNCs), octahedra (PdOCTs) and cuboctahedra (PdCUOCs).<sup>51</sup> Intriguingly the authors found that nanocatalysts containing the smallest number of edge and corner atoms (PdNCs) proved the most active in this reaction (**Figure 6a**), suggesting a link between activity and the presence of Pd (100) surface facets, rather than the defect sites highlighted *vide supra*. This was further investigated through use of both 10 nm and 20 nm PdNCs (**Figure 6b**), the larger particles possessing a much smaller percentage of edge and corner atoms (0.16% for a 20 nm cube compared to 0.4% for a 10 nm cube). Almost identical reaction profiles for the different PdNCs were obtained, with the Pd concentration adjusted to allow for the same number of surface Pd atoms.

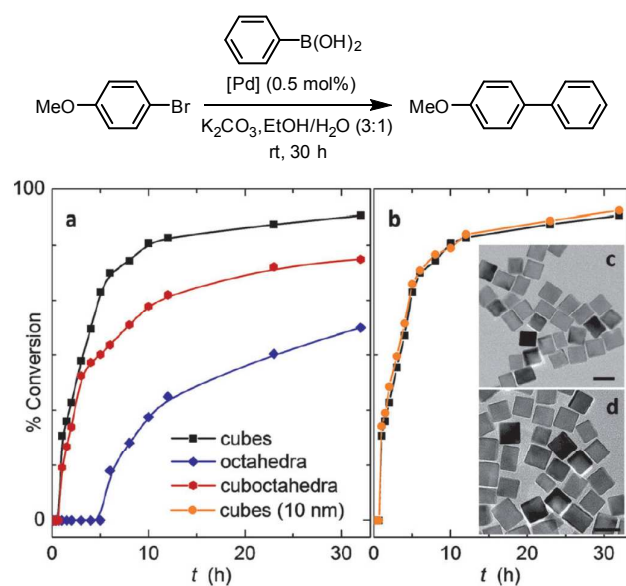


**Figure 6.** Shape sensitivity in a Suzuki–Miyaura coupling catalysed by Pd nanocatalysts with defined surface facets (McGlacken *et al.*, 2014).<sup>51</sup> Reproduced with permission from *Angew. Chem. Int. Ed.*, 2014, 53, 4142. Copyright 2014 WILEY-VCH Verlag GmbH & Co.

This difference in reactivity was ascribed to preferential leaching from the (100) facets of PdNCs, promoted by oxidative etching from O<sub>2</sub>. TEM analysis of the nanocatalysts used appeared to show shape distortions resulting from the reaction conditions, while inductively coupled plasma mass spectrometry (ICP-MS) showed the presence of leached Pd in the post-reaction mixtures of all the nanocatalysts used. Greater quantities of leached Pd were found in those reactions which contained PdNCs. Critically this study indicates that the proposed oxidative etching is shape sensitive in nature and that the reaction likely proceeds *via* a (quasi)homogeneous catalytic cycle. It is interesting to note the perceived difference between a heterogeneous and homogeneous manifold in two very similar reactions (**Figure 4** and **Figure 6**); possibly this results from the different quantities of O<sub>2</sub> present in these reactions, however it is likely that stabilisation of the PdNPs by PVP in the former example plays a key role.

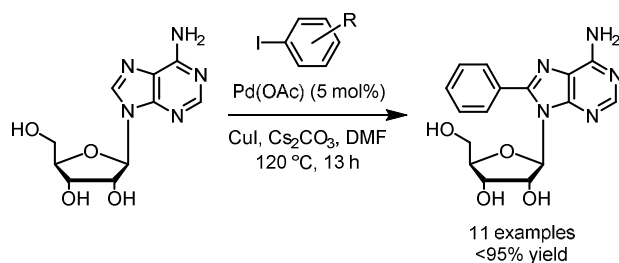
A study on the stability of PVP-Pd catalysts shows that for those particles with low-index surfaces, high energy facets such as the (110) present in PdNCs are the least stable due to their preferential susceptibility to oxidation, while octahedral particles containing mostly (111) facets display correspondingly greater stability. Conversely those particles with high-index surfaces, such as concave nanocubes (PdCNCs), display superior stability due to stronger chemisorption to the PVP polymer.<sup>52</sup> Notably the particles used in the study by Fairlamb *et al.* consist of PVP-capped truncated cuboctahedra, which presents an interesting explanation for the mechanistic dichotomy observed. Work by McGlacken and co-workers extended this concept when examining the use of high-index PdCNCs in a similar Suzuki–Miyaura couplings. In the absence of a stabilising agent such as PVP, the (730) facets present in PdCNCs resulted in greater leaching and thus higher activity when compared to the low-index (100) facets present in PdNCs.<sup>53</sup>

## The relevance of Pd nanoparticles as active catalysts in C–H bond functionalisations

### Degradation (activation) of Pd(OAc)<sub>2</sub>

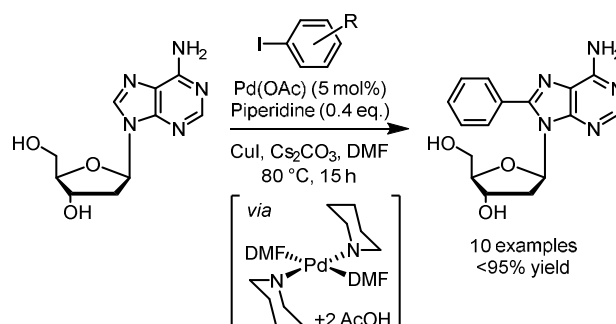
As with the traditional cross-coupling reactions detailed above, it is important to recognise that common Pd (pre)catalysts can often act as Pd reservoirs for the subsequent generation of Pd<sup>0</sup> particles, or indeed as PdNP sources in their own right. During our group's development of conditions for the direct C8-arylation of the purine nucleoside adenosine (**Scheme 3**),<sup>54</sup> it was observed that agglomerates of insoluble Pd black were formed rapidly from Pd(OAc)<sub>2</sub> (note: that this precursor complex usually derives from Pd<sub>3</sub>(OAc)<sub>6</sub>) under the reaction conditions employed. In these studies, the formation of Pd/Cu-containing nanoparticles was also observed during substrate turnover. TEM analysis of the reaction mixture demonstrated

the formation of 3 nm PdNPs during the latter stages of the reaction. This analysis was conducted using a method developed to trap PdNPs that are generated *in situ*, through addition of 10 monomer equivalents of exogenous PVP polymer to an aliquot of the reaction mixture. This polymer acts as a stabiliser for the particles,<sup>49, 50</sup> ensuring that they are not modified by solvent removal or other techniques employed in the preparation of the sample for TEM, thus enabling more accurate characterisation of the reactive particles. Subsequent investigation of several soluble Pd sources produced the same observation, while maintaining equivalent levels of substrate conversion. Correspondingly insoluble Pd sources such as Pd(OH)<sub>2</sub>/C and PVP-Pd also functioned as an effective catalyst for this reaction, although the use of high temperatures and DMF (a highly palladophilic solvent) appeared to result in extensive leaching from these nominally heterogeneous Pd sources, producing a quasi-homogeneous catalytic manifold.<sup>54</sup>



**Scheme 3.** Direct C8-arylation of adenosine using Pd(OAc)<sub>2</sub> (Fairlamb *et al.*, 2008).<sup>54</sup>

During subsequent studies on the direct C8-arylation of the more sensitive 2'-deoxyadenosine substrate (**Scheme 4**),<sup>55</sup> the previously observed Pd/Cu nanoparticles were shown to be critical to precatalyst activation. Trace levels of dimethylamine impurities in the DMF used for this reaction were found necessary for effective substrate turnover. Screening of several amine additives in this reaction revealed that piperidine was able to produce a similar effect; preparation of the corresponding *trans*-Pd(OAc)<sub>2</sub>(piperidine)<sub>2</sub> catalyst allowed for a more detailed investigation of this phenomenon. This catalyst was observed to rapidly degrade to form well-defined 1.7 nm DMF-PdNPs under the reaction conditions (80 °C), *via* a Pd(piperidine)<sub>2</sub>(DMF)<sub>2</sub> complex. More recently, Obora and co-workers have prepared stabilised forms of both DMF-PdNPs and DMF-Cu/PdNPs.<sup>56-58</sup> Alami *et al.* have also performed the direct C8-arylation of adenines mediated by Pearlman's catalyst (Pd(OH)<sub>2</sub>/C) at elevated temperatures in polar aprotic solvents such as DMF and NMP.<sup>59, 60</sup> No specific mention of Pd speciation is made, however this likely occurs under these conditions (see example by Fagnou *et al.*, **Scheme 11**).<sup>61</sup>

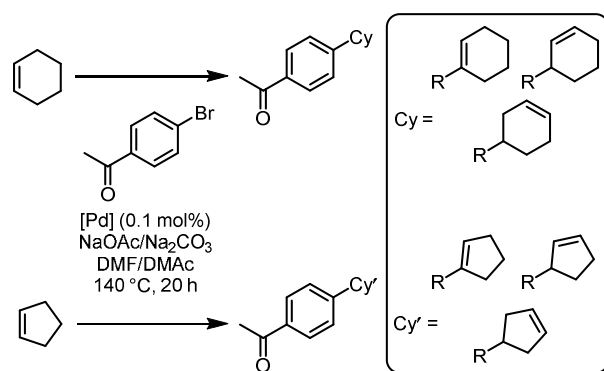


**Scheme 4.** Direct C8-arylation of 2'-deoxyadenosine *via* a Pd<sup>II</sup>-piperidine complex forming DMF-PdNPs *in situ* (Fairlamb *et al.*, 2009).<sup>55</sup>

### The importance of polar solvents for PdNP proliferation

Such evidence of DMF-stabilised PdNPs makes it clear that solvent effects can prove non-innocent with regards to the nature of the active catalyst formed in many reactions. The solvent must therefore be considered as an intrinsic mechanistic factor. Work by Hii and co-workers<sup>62</sup> on the speciation of Pd(OAc)<sub>2</sub> in a Suzuki–Miyaura reaction allowed the potential factors affecting the catalyst activation process to be investigated. It was found that water specifically effects a rapid hydrolytic dissociation of the Pd<sub>3</sub>(OAc)<sub>6</sub> trimer cluster to create an intermediate species, which is subsequently reduced to Pd<sup>0</sup> (in this case by arylboronic acids). The quantity of water present thus specifically controls the amount of catalytically relevant Pd<sup>0</sup> available in the reaction mixture. Furthermore, the nuclearity of Pd(OAc)<sub>2</sub> appeared to be directly correlated to the dipole moment of the solvent of choice and more independent of the dielectric constant. Polar aprotic solvents with large dipole moments such as DMF will therefore result in a greater degree of dissociation of Pd(OAc)<sub>2</sub> (as was indirectly observed in our work detailed above) than those with small dipole moments, such as toluene.

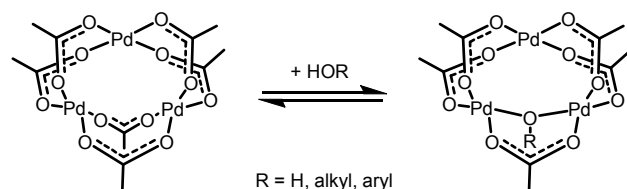
A method of probing the heterogeneity of Heck reactions performed in polar aprotic solvents at elevated temperatures has been developed by Djakovitch and co-workers.<sup>63</sup> They found that product selectivity when using cyclic alkenes is strongly dependent on the nature of the catalytic Pd species involved (**Scheme 5**). Specifically, in their Heck coupling the most active Pd species are solubilised molecular Pd, while reaction on the surface of metallic Pd promotes dehalogenation. They concluded that concurrent homogeneous and heterogeneous manifolds are therefore in operation. Choi *et al.* have also documented a HPLC-MS technique to allow detection of ultra-small DMF-PdNPs, which might have passed unobserved by other analytical methods such as TEM.<sup>64</sup>



**Scheme 5.** Heck reaction using cyclic alkenes as a probe for detection of homogeneous vs. heterogeneous Pd species (Djakovitch *et al.*, 2004).<sup>63</sup>

The degradation of  $\text{Pd}(\text{OAc})_2$  and  $\text{Pd}_2(\text{dba})_3$  has been utilised by Gómez *et al.* to produce PdNPs of ca. 2 nm, stabilised by imidazolium-containing ionic liquids<sup>65</sup> (drawing comparison with the earlier work by Dupont and co-workers),<sup>43</sup> while propagation of PdNPs from  $\text{Pd}(\text{OAc})_2$  in DMF has also been observed by Ranu *et al.* in the direct acylation of aryl halides<sup>66</sup> and the direct arylation of benzothiazole.<sup>67</sup> This effect was also noted by Langer and co-workers in the direct arylation of pyrroles performed in ionic liquids at elevated temperatures. This protocol was shown to be effective when catalysed by preformed PVP-supported PdNPs of around 1–2 nm.<sup>68</sup> Felpin and co-workers added charcoal as a stabiliser for PdNPs formed *in situ* from  $\text{Pd}(\text{OAc})_2$  in their direct intramolecular formation of phenanthrenes from stilbenes, with ICP-MS of the post-reaction mixtures used to highlight the affinity of charcoal for these catalytic Pd species.<sup>69</sup> Ananikov and co-workers have also gained detailed insight into the degradation behaviour of  $\text{Pd}_2(\text{dba})_3$  in chloroform,<sup>70</sup> demonstrating an efficient capture mechanism of the resultant PdNPs by activated carbon at 40 °C. By using these reactive Pd markers, they were able to demonstrate >2000 reactive centres per 1  $\mu\text{m}^2$  of carbon surface area.<sup>71</sup>

More recently, Bedford and co-workers have demonstrated the facile hydrolysis and alcoholysis of  $\text{Pd}(\text{OAc})_2$  (from its native trimeric form,  $\text{Pd}_3(\text{OAc})_6$ ).<sup>72</sup> Their work makes clear that in any catalytic process utilising  $\text{Pd}(\text{OAc})_2$ , intermediates such as those shown in **Scheme 6** should be considered as relevant species. Furthermore,  $\text{Pd}(\text{OAc})_2$  must be viewed as a highly labile (pre)catalyst in solution.

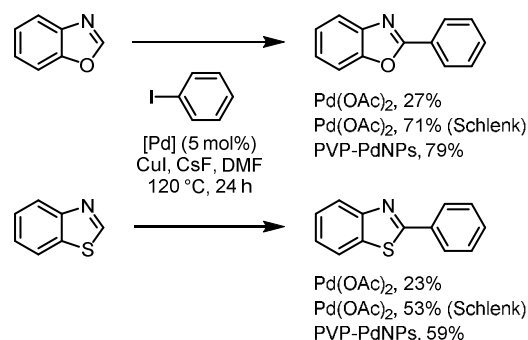


**Scheme 6.** Equilibrium between  $\text{Pd}_3(\text{OAc})_6$  trimer and  $\mu^2$ -hydroxide or alkoxide species (Bedford *et al.*, 2015).<sup>72</sup>

### Propagation of PdNPs in C–H bond functionalisations

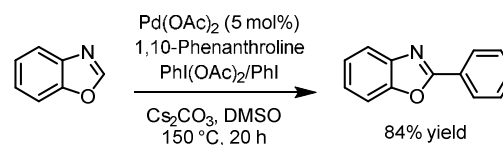
Our group has established that considerations regarding the activation of  $\text{Pd}(\text{OAc})_2$  and other related precursors to form well-defined PdNPs can also be extended to several C–H bond functionalisation protocols, allowing for the activity of pre-synthesised PdNP catalysts to be independently tested and compared in these reactions.<sup>73</sup> For example under the conditions detailed in **Scheme 4**, use of a stabilised PVP-PdNP catalyst allowed for the reaction temperature to be lowered to 60 °C, with no appreciable decrease in conversion.

During studies on the direct C2-arylation of benzoxazole and benzothiazole under the Pd/Cu-catalysed conditions shown in **Scheme 7**, a significant deleterious air effect was noted on the reaction when using  $\text{Pd}(\text{OAc})_2$  as the catalyst. If however pre-synthesised PVP-PdNPs were used, rigorous exclusion of air was not required to obtain similar yields of the desired 2-aryl products.



**Scheme 7.** Direct C2-arylation of benzoxazole and benzothiazole using  $\text{Pd}(\text{OAc})_2$ -derived *in situ* and supported PdNPs (Fairlamb *et al.*, 2014).<sup>73</sup>

TEM analysis of the reaction mixture using our previously developed sampling technique<sup>54</sup> revealed that the PdNPs generated from  $\text{Pd}(\text{OAc})_2$  under Schlenk conditions were larger and more varied in size than those generated when air was not rigorously excluded. This led to the conclusion that these larger particles formed in the absence of air, and were also more active under the reaction conditions. Interestingly however, the pre-synthesised PVP-PdNPs which evidenced equivalent activity, without rigorous exclusion of air, were smaller than those generated from  $\text{Pd}(\text{OAc})_2$ . The PVP polymer may therefore be preventing oxidative Pd leaching in this example (see study on PVP-PdNP stability by McGlacken *et al.*<sup>51</sup> above). Other conditions for the selective C2-arylation of benzoxazole were also investigated to determine the potential involvement of PdNPs in a reported  $\text{Pd}^{\text{II/IV}}$  catalytic manifold (**Scheme 8**).



**Scheme 8.** Direct C2-arylation of benzoxazole with  $\text{PhI}(\text{OAc})_2$  or  $\text{PhI}$  (Fairlamb *et al.*, 2013).<sup>74</sup>

The literature conditions for this process necessitated the use of a hypervalent iodine reagent,  $\text{PhI}(\text{OAc})_2$ , as the aryl coupling partner. The similarity to our conditions using iodobenzene and DMF however prompted us to further examine the behaviour of the Pd catalyst. Upon addition of DMSO to the reaction mixture, a clear colour change to the dark brown of colloidal PdNPs was observed. TEM analysis of this reaction mixture demonstrated PdNPs that were uniformly <5 nm in size, which suggested that  $\text{Pd}^0$  species were catalytically relevant under these conditions (Figure 7). Subsequently, it was found that  $\text{PhI}(\text{OAc})_2$  rapidly degrades to PhI within 10 mins at 150 °C in DMSO; correspondingly, use of PhI as the aryl coupling partner in place of the oxidising  $\text{PhI}(\text{OAc})_2$  had no effect on the yield of the reaction. In light of these findings it was proposed that this reaction does in fact proceed through a  $\text{Pd}^{0/\text{II}}$  manifold, where PdNPs propagated from the degradation of  $\text{Pd}(\text{OAc})_2$  are key catalytic species.<sup>74</sup>

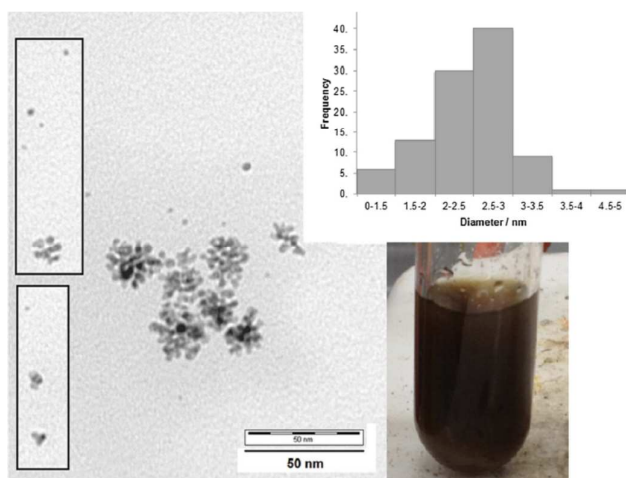
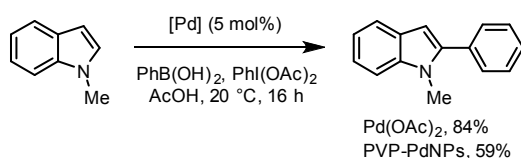


Figure 7. PdNPs formed *in situ* from the reduction of  $\text{Pd}(\text{OAc})_2$  in DMSO for the direct C2-arylation of benzoxazole (Fairlamb *et al.*, 2013).<sup>74</sup> Reprinted from *Tetrahedron*, 2014, 70, 6174, Copyright 2014, with permission from Elsevier.

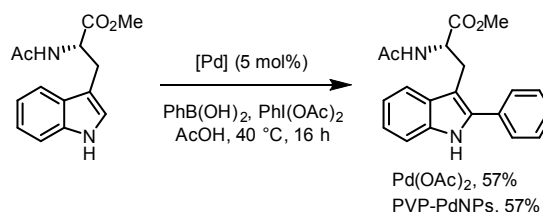
More recently, Sanford's conditions for the direct C2-arylation of *N*-methylindole with phenylboronic acid and iodobenzene in acetic acid were explored.<sup>75</sup> It was noted that PdNPs were visibly formed within seconds of substrate addition, so PVP-Pd was utilised as a catalyst for this reaction and provided the desired aryl product in 59% yield (Scheme 9).



Scheme 9. Direct C2-arylation of *N*-methylindole using  $\text{Pd}(\text{OAc})_2$  (Sanford *et al.*, 2006)<sup>75</sup> and PVP-PdNPs (Fairlamb *et al.*, 2014).<sup>73</sup>

This methodology was subsequently applied to the direct C2-arylation of a protected tryptophan derivative,<sup>76, 77</sup> whereupon the rapid propagation of PdNPs was observed within minutes. TEM analysis of the reaction mixture highlighted the presence

of AcOH- and PVP-stabilised nanoparticles; as with the direct arylation of benzoxazole, these particles were uniformly <5 nm in size. Once again, a PVP-Pd catalyst demonstrated equivalent activity in this transformation (Scheme 10).



Scheme 10. Direct C2-arylation of a tryptophan derivative using  $\text{Pd}(\text{OAc})_2$ -derived *in situ* and supported PdNPs (Fairlamb *et al.*, 2014).<sup>76</sup>

The examples highlighted above establish that in many reactions, propagation of PdNPs from common Pd precursors to form catalytically competent  $\text{Pd}^0$  species, is a crucial factor. Moreover, pre-supported PdNP catalysts such as PVP-Pd are a demonstrably viable catalyst for many C–H bond functionalisation protocols. The use of such catalysts allows for a greater degree of control over potentially complex catalytic manifolds, where a multi-ensemble of higher order Pd species often play a key role.

## Activity of supported Pd nanoparticles in C–H bond functionalisation chemistry

### Background

To date there are only a handful of supported Pd nanoparticulate catalysts that have been described in the literature for use in C–H bond functionalisation chemistry,<sup>78, 79</sup> in contrast to more traditional Pd-catalysed cross-coupling reactions.<sup>11–14</sup> Despite their limited number these catalysts are highly varied and correspondingly they display diverse reactivities. Interestingly both  $\text{Pd}^0$  and  $\text{Pd}^{\text{II}}$  supported species are reported, although proposed mechanisms understandably centre on  $\text{Pd}^0/\text{Pd}^{\text{II}}$  manifolds; external oxidants are often employed however, allowing for higher oxidation state manifolds to be potentially accessed. A common feature of these catalytic systems is their low Pd loadings, typically resulting from a heterogeneous system where extensive Pd leaching is not observed. This naturally allows for a more effective use of this precious metal catalyst, with some exceptions (*vide infra*). A wide range of organic and inorganic supports have been utilised for the preparation of these species, which have been broadly grouped together into similar classes for the purposes of this article.

### Commonly employed heterogeneity tests

The work highlighted in this article and others<sup>33–36, 80–82</sup> makes it clear that determining the extent of homogeneous vs. heterogeneous catalysis in a given system is often a difficult task, made more so by the lack of any single absolute empirical test for the confirmation of the true nature of the catalytically competent metal species. In many of the examples discussed

below, a plethora of tests to indicate proposed heterogeneous behaviour are utilised; for ease these are summarised here and referred to in brief for each example highlighted.

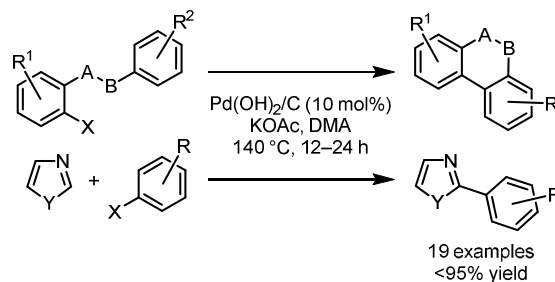
The 'Hg drop test' involves the addition of a large excess (*ca.* 200–500 eq.) of elemental Hg to a reaction mixture, both from the start of a reaction and more commonly, during active turnover of the catalyst under normal working conditions. Hg has been shown to inhibit surface reactions through poisoning of the catalyst; this is believed to occur as a result of surface amalgamation of the mercury with any heterogeneous particles present in the reaction mixture. Addition of mercury to a catalytically relevant metal nanoparticle will therefore retard the ability of such particles to effectively catalyse reactions.<sup>83</sup> A positive result indicates that after addition of Hg, substrate turnover ceases. It is important to note however that due to the high density of elemental Hg, stirring efficiency can have a pronounced effect on the dispersion of the metal throughout the reaction, thus affecting the reliability of this test.

The hot filtration test is applied by filtering the entire reaction mixture through a pre-heated Celite pad (or other diatomaceous metal scavenger) during catalyst turnover. Any nanoparticulate metal species would in theory be filtered out of the mixture by this process, whereas soluble mononuclear species would pass through. Any heterogeneous bases or reagents (*e.g.* K<sub>2</sub>CO<sub>3</sub>) are recharged and the reaction is continued under normal conditions. A positive result indicates that after filtration, substrate turnover ceases. This test cannot however isolate very small and/or solubilised nanoparticles.

The three-phase test comprises a solid-supported substrate (immobilised on a non-reactive polymer *e.g.* Wang resin) used in place of the normal substrate, with analysis of both reaction mixture and solid support at the end of the reaction to test for leaching. Active homogeneous catalyst species should be able to access the supported substrate and produce solid-supported product under the normal reaction conditions. If the active catalyst is heterogeneous however, it should be unable to interact sufficiently with the encapsulated substrate and provide little or no observable product. It is of course possible that inactive homogeneous particles could be formed *via* leaching, analytical measurements such as ICP-MS can be used to test for this scenario. In order to maintain appropriate scientific rigour, several variants of this basic test are normally performed as control experiments. Typically, the following scenarios are required: (1) normal reaction conditions with solid support added to test for reaction inhibition by the polymer, (2) reaction using both supported and unsupported substrate to observe whether product is formed in solution or on the polymer (or both), (3) reaction using only solid-supported substrate to observe whether product is formed in solution or on the polymer. A positive result for heterogeneous catalytic behaviour would indicate: (1) normal conversion, (2) product seen only in solution, (3) no product observed either on the support or in solution (which would indicate leaching).

The use of resins to distinguish between homogeneous and heterogeneous manifolds is not without its complications

however. Fagnou and co-workers utilised this approach when investigating intra- and intermolecular direct arylation reactions mediated by Pd(OH)<sub>2</sub>/C (Scheme 11).<sup>61</sup> In their case, anchoring of an aryl halide to Wang resin afforded complete conversion to the desired cyclic product, potentially indicating a homogeneous process as a result of Pd leaching.



**Scheme 11.** Direct intra- and intermolecular arylation reactions using Pd(OH)<sub>2</sub>/C (Fagnou *et al.*, 2005).<sup>61</sup>

This experiment does not however confirm whether the active catalytic species are mononuclear Pd or small Pd clusters, as the pore size of Wang resin is sufficiently large as to allow seeding and encapsulation of multinuclear clusters. It has for example been shown that thiolated resins such as Quadrasil-MP, in addition to unfunctionalised mesoporous silicas, are capable of sequestering PdNPs (Figure 8);<sup>48</sup> such supports therefore cannot be considered selective for soluble Pd. Hazrati and co-workers have also used Pd(OH)<sub>2</sub>/C to effect the direct C2-arylation of pyrroles at elevated temperatures in triethanolamine, conditions which likely produce similar Pd speciation.<sup>84</sup> Other tests for heterogeneity often used in addition to the methods detailed above are: a) characterisation of the prepared catalysts before and after use; b) analysis of the metal content of the post-reaction mixture, and c) catalyst recyclability studies.

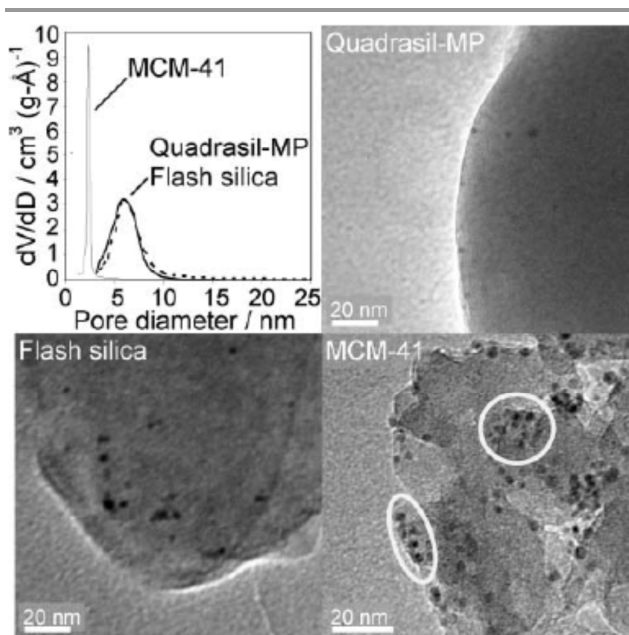
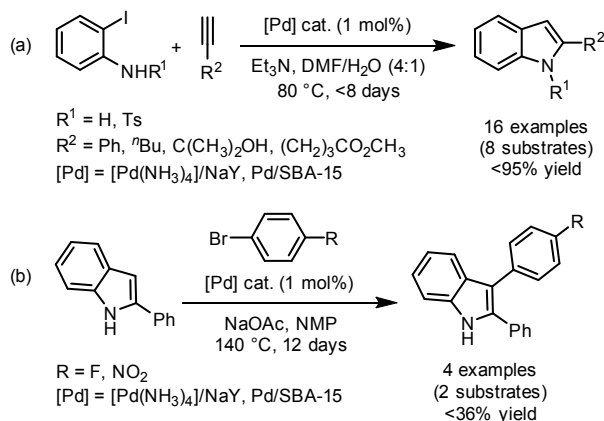


**Figure 8.** TEM images evidencing encapsulation of PdNPs within mesoporous silicas and their associated pore-size distributions (Fairlamb *et al.*, 2010).<sup>48</sup> Reproduced from Ref 48 with permission from The Royal Society of Chemistry.

### Metal–metal frameworks

One of the largest classes of supported Pd nanocatalysts are metal–metal frameworks incorporating the catalytic Pd source with at least one other metal. An early demonstration of this approach by Djakovitch and co-workers reported the construction of C2-functionalised indoles (**Scheme 12a**) and their subsequent C3-arylation (**Scheme 12b**).<sup>85</sup>

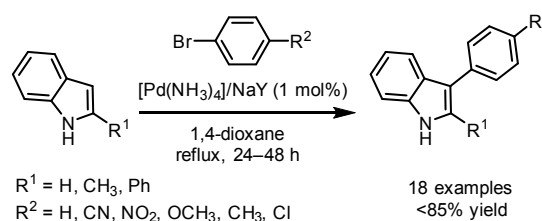


**Scheme 12.** Construction of C2-functionalised indoles and their subsequent C3-arylation using microporous and mesoporous Pd catalysts (Djakovitch *et al.*, 2006).<sup>85</sup>

This was achieved using both a microporous Pd nanocomposite  $[\text{Pd}(\text{NH}_3)_4]/\text{NaY}$ , prepared by ion exchange from a NaY zeolite and a mesoporous silica-based catalyst Pd/SBA-15, prepared by grafting of a Pd-alkoxide catalyst into the pores of a calcined silica (SBA-15). While both catalysts performed equally well in the construction of C2-indoles (**Scheme 12a**), the mesoporous Pd/SBA-15 proved much more

effective in the subsequent C3-arylation (**Scheme 12b**). Recyclability and leaching experiments for the reaction shown in **Scheme 12a** indicated that for the microporous  $[\text{Pd}(\text{NH}_3)_4]/\text{NaY}$  catalyst, leaching was extensive and led to a rapid drop-off in conversion upon catalyst reuse. This is to be expected under such forcing conditions (high temperatures, excessive reaction times) in palladophilic solvents such as DMF. Interestingly, this was not observed for the mesoporous Pd/SBA-15 catalyst, which demonstrated very little leaching of Pd into solution, possibly indicating a more heterogeneous catalytic manifold.

Subsequent work from the same group established the first completely selective heterogeneously catalysed C3-arylation of C2-substituted, free N-H indoles (**Scheme 13**) using the Pd nanocomposite,  $[\text{Pd}(\text{NH}_3)_4]/\text{NaY}$ .<sup>86</sup> The authors demonstrated that 1 mol% of this heterogeneous catalyst affords the desired products in similar conversions to those when using 5 mol% of  $\text{Pd}(\text{OAc})_2$ , an observation accounted for by the formation of catalytically inactive Pd black in the latter case. Iodobenzene substrates were incompatible with this system; surprisingly this was not due to homocoupling to produce biphenyl derivatives, as anticipated, but rather because dehalogenation to produce the corresponding benzene derivatives was observed in significant yields (>20%). This may hint at the halide-capturing ability of the nanocomposite, drawing interesting comparisons to commonly utilised Ag salts, often proposed to act as halide scavengers in other C–H bond functionalisation protocols.<sup>87</sup>



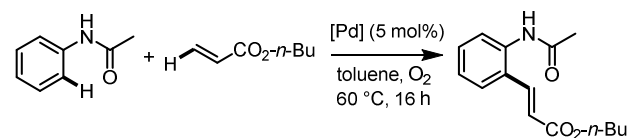
**Scheme 13.** Selective C3-arylation of C2-substituted indoles using a Pd/NaY catalyst (Djakovitch *et al.*, 2008).<sup>86</sup>

Surprisingly, this catalyst also appeared to be highly selective for the C3 position of indole, as no migration to the C2 position to produce 2-phenylindole was observed (as would often be the case with homogeneous Pd manifolds). In general, electron-rich aryl bromides gave higher yields of the desired products than electron-deficient examples.

Ying and co-workers have investigated the use of Pd-polyoxometalate (POM) nanomaterials supported on carbon with the general formula  $\text{Pd-PV}_x\text{Mo}_y/\text{C}$  ( $x = 0-3$ ,  $y = 12-9$ ), where the composite material can act as an electron-transfer mediator for re-oxidation of the heterogeneous Pd source ( $\text{O}_2$  is used as a terminal oxidant).<sup>88</sup> These materials were prepared by reduction of a  $\text{Pd}(\text{NO}_3)_2$  salt with  $\text{NaBH}_4$  in the presence of a carbon support and the appropriate POM, which also provides a suitable capping agent during the synthesis of the PdNPs, ensuring that they are uniform and well-dispersed with diameters of 2–3 nm (in contrast to particles formed in the

absence of POM). These catalysts were subsequently evaluated in the C–C bond-forming reaction between acetanilide and *n*-butyl acrylate in which the Pd–PV<sub>3</sub>Mo<sub>9</sub>/C catalyst was found to give the highest yield by a small margin (**Table 1, Entry 4**).

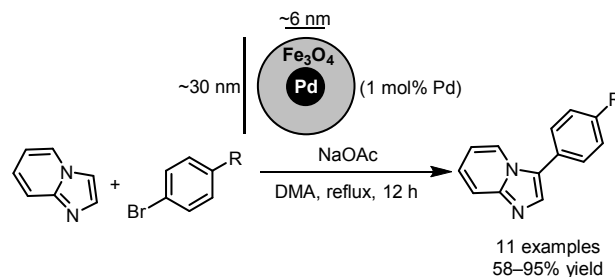
**Table 1.** Catalytic activity of Pd-POM nanomaterials in the oxidative reaction between acetanilide and *n*-butylacrylate (Ying *et al.*, 2011).<sup>88</sup>



Entry	Catalyst	Pd (wt%)	POM (wt%)	Yield (%)
1	Pd-PMo <sub>12</sub> /C	8.1	15.2	44
2	Pd-PV <sub>1</sub> Mo <sub>11</sub> /C	12.5	15.1	39
3	Pd-PV <sub>2</sub> Mo <sub>10</sub> /C	10.4	14.8	41
4	Pd-PV <sub>3</sub> Mo <sub>9</sub> /C	7.9	15.2	54
5	Pd/C	17.0	0.0	0
6	Pd/C + PV <sub>3</sub> Mo <sub>9</sub>	17.0	0.0	9

While not commented on by the authors, it appears that there was a slight negative correlation between the Pd loading of the POM catalysts and the yield observed in this reaction (*i.e.* lower Pd loadings by weight in the POM gave a higher yield, all reactions contained 5 mol% Pd). Increasing the temperature to 80 °C allowed the desired product to be obtained in an isolated yield of 76%. The recyclability of the Pd–PV<sub>3</sub>Mo<sub>9</sub>/C catalyst was also investigated, whereupon it was discovered that significant POM losses (54%) occurred under the reaction conditions; recovery of the catalyst by centrifugation and reuse resulted in a large drop in product yield (by 23%). If however the catalyst was recovered and reloaded with POM prior to reuse the catalyst retained 97% activity after one use, and 79% after three uses.

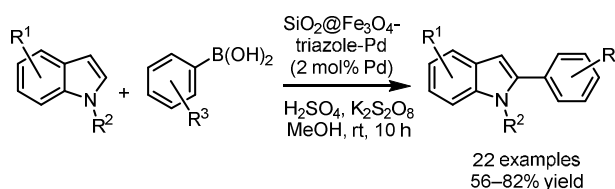
Exploration of other methods for the recovery of these precious metal catalysts has demonstrated that magnetism can provide an operationally simple process for catalyst recycling. Lee *et al.* have reported the direct C3-arylation of imidazo[1,2-*a*]pyridine with aryl bromides, mediated by a magnetically recoverable Pd–Fe<sub>3</sub>O<sub>4</sub> nanoparticle catalyst (**Scheme 14**).<sup>89</sup>



**Scheme 14.** Direct C3-arylation of imidazo[1,2-*a*]pyridine using a magnetically recoverable Pd–Fe<sub>3</sub>O<sub>4</sub> nanocatalyst (Lee *et al.*, 2013).<sup>89</sup>

Following the direct arylation protocol, isolation of the catalyst using a neodymium magnet followed by washing allowed for up to 98% of the catalyst to be recovered. Impressively, the recovered catalyst demonstrated identical catalytic activity under the conditions shown in **Scheme 14** even after ten recovery/reuse cycles.

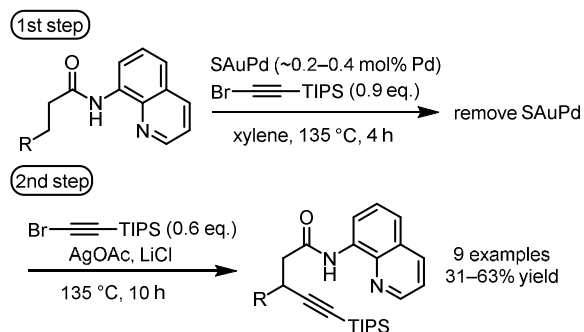
Along similar lines, Wang and co-workers have utilised silica-coated Fe<sub>3</sub>O<sub>4</sub> nanoparticles (SiO<sub>2</sub>@Fe<sub>3</sub>O<sub>4</sub>) to generate immobilised, magnetically recoverable Pd<sup>II</sup> nanoparticulate catalysts *via* an azide-promoted “click” reaction to give the key 1,4-substituted 1,2,3-triazole linker which acts as a monodentate ligand for Pd<sup>II</sup> (obtained from Pd(OAc)<sub>2</sub>).<sup>90</sup> These SiO<sub>2</sub>@Fe<sub>3</sub>O<sub>4</sub>-triazole-Pd particles had good size uniformity, with an average diameter of 140 nm. The prepared catalysts demonstrated good activity in the direct C2-arylation of a range of indoles with aryl boronic acids, although requiring the use of an acidic additive (H<sub>2</sub>SO<sub>4</sub>) and molecular oxidant (K<sub>2</sub>S<sub>2</sub>O<sub>8</sub>) (**Scheme 15**).



**Scheme 15.** Direct C2-arylation of indoles with aryl boronic acids using a magnetically recoverable, silica coated Pd<sup>II</sup> nanocatalyst (Wang *et al.*, 2014).<sup>90</sup>

*N*-methyl protected indoles proved the most effective in this protocol, electron-deficient indoles gave lower yields but a variety of aryl boronic acids (electron-rich, electron-poor and sterically hindered) were well tolerated. As with the previous example, after magnetic recovery and washing these catalysts demonstrated excellent recyclability, with a decrease in yield of only 5% after eight uses. ICP analysis also demonstrated that catalyst leaching was not an issue for this system, as the post-reaction mixture contained less than 0.20 ppm Pd.

Arisawa and co-workers have developed a sulfur-modified Au-supported Pd catalyst, SAuPd, prepared by heating of the SAu material in the presence of Pd(OAc)<sub>2</sub> to afford surface-bound PdNPs of *ca.* 5 nm.<sup>91</sup> This was demonstrated to effectively catalyse the alkylation of a range of aliphatic amides all containing an 8-aminoquinoline directing group with a TIPS-protected bromoalkyne (**Scheme 16**).



**Scheme 16.** Alkynylation of an aliphatic amide using a sulfur-modified Au-supported Pd catalyst (Arisawa *et al.*, 2014).<sup>91</sup>

This reaction required extensive optimisation; LiCl was found to inhibit formation of the dialkynylated product (albeit with reduced yield of the desired monoalkynylated product), AgOAc was effective as a oxidant but caused uncontrolled leaching of Pd into the reaction mixture, hence the reaction was divided into two steps with the SAuPd removed prior to addition of the AgOAc and LiCl. The catalytically active species under these conditions appears to be Pd<sup>II</sup>; this species has difficulty returning to the SAu surface following leaching, controlling the rate of leaching was therefore critical for catalyst recyclability. ICP-MS analysis of the reaction mixture and the SAuPd catalyst before and after each reaction was used to determine the extent of leaching and it was found that the catalyst could be recycled and reused up to ten times, although by the tenth reuse the yield had significantly dropped (to 14% from 53%); a more realistic recycle rate would be five times as the yield had decreased by only 7% at this point (**Table 2**). Inductively coupled plasma mass spectrometry (ICP-MS) performed on the post-reaction mixture show that this corresponds to decreasing amounts of Pd available for the reaction with each reuse (*i.e.* lower catalyst loadings). This catalytic system is therefore interesting because it does not preclude leaching, rather it has been tailored to make effective use of a system where leaching cannot be controlled (if the desired product is to be formed).

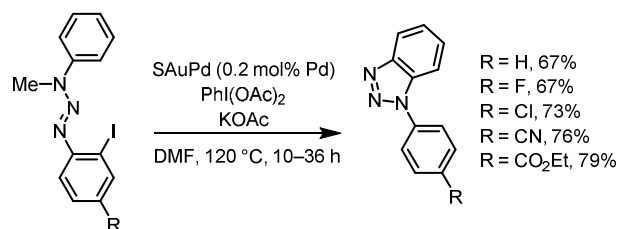
**Table 2.** Quantity of Pd found in post-reaction mixture after ten cycles of the directed alkynylation of an amide using SAuPd (Arisawa *et al.*, 2014).<sup>91</sup>

Entry/Reaction Cycle	Leached Pd (ppm, mmol%) <sup>[a]</sup>	Yield (%)
1	1710 ± 327 (10, 8)	53
2	1203 ± 510 (7, 5)	51
3	906 ± 622 (5, 4)	50
4	570 ± 217 (3, 3)	49

5	743 ± 448 (4, 3)	46
6	570 ± 216 (3, 3)	40
7	303 ± 118 (2, 2)	36
8	480 ± 108 (3, 3)	31
9	323 ± 115 (2, 2)	23
10	233 ± 110 (1, 1)	14

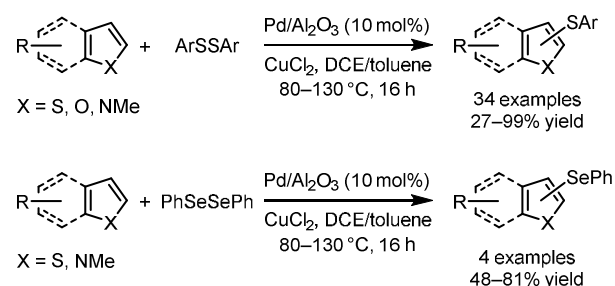
<sup>[a]</sup> Leached Pd in ng

A subsequent publication from the same group utilised the SAuPd catalyst for the synthesis of *N*-substituted benzotriazoles *via* a succinct Pd-mediated 1,7-migration/cyclization/dealkylation sequence (**Scheme 17**).<sup>92</sup> It should be noted that a molecular oxidant was again required for this transformation, hinting at the involvement of a catalytically relevant Pd<sup>II</sup> species.



**Scheme 17.** Synthesis of *N*-substituted benzotriazoles using a sulphur-modified Au-supported Pd catalyst (Arisawa *et al.*, 2014).<sup>92</sup>

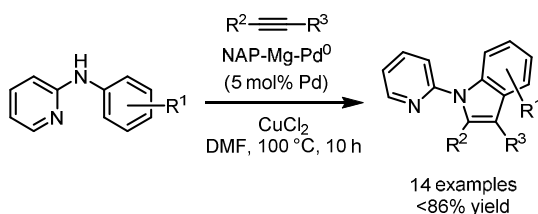
Glorius and co-workers have demonstrated the efficacy of alumina-supported Pd (Pd/Al<sub>2</sub>O<sub>3</sub>) in the direct thiolation and selenation of electron-rich heteroarenes (**Scheme 18**).<sup>93</sup> The heterogeneous catalysts Pd/C, Pd/SiO<sub>2</sub> and Pd(OH)<sub>2</sub>/C also demonstrated some activity for this transformation. High selectivity was observed for reaction at the C5 position (C3 for 6,5-ring systems) over the C3 position (C2 for 6,5-ring systems). A broad range of thiophenes containing electron-donating and electron-withdrawing groups were tolerated, although increased yields were observed for those electron-donating examples. Correspondingly, electron-rich disulfides exhibited higher reactivities than electron-poor examples.



**Scheme 18.** Direct thiolation and selenation of electron-rich heterocycles using Pd/Al<sub>2</sub>O<sub>3</sub> (Glorius *et al.*, 2015).<sup>93</sup>

Several synthetic protocols were employed to test the heterogeneity of this reaction. The concentration of Cu and Pd in solution after 16 h under the reaction conditions was measured by Total reflection X-ray fluorescence (TXRF); in toluene <80 ppm Cu and <5000 ppm Pd were found, in DCE 440 ppm of Cu and 234,000 ppm Pd were found, after centrifugation values of <80 ppm Cu and <5000 ppm Pd were obtained. Despite these seemingly large values for leached Pd, the hot filtration test showed no further conversion to product after filtration and the three-phase test demonstrated that no active homogeneous palladium species were formed under the reaction conditions. The authors also note that the reaction was dependent on rapid stirring rates, again suggesting heterogeneous catalytic behaviour. Perhaps because of extensive leaching, the Pd/Al<sub>2</sub>O<sub>3</sub> catalyst demonstrated poor recyclability in this system, with yields of 63% and 42% being obtained for the second and third catalyst cycles, respectively (cf. 75% for the first cycle).

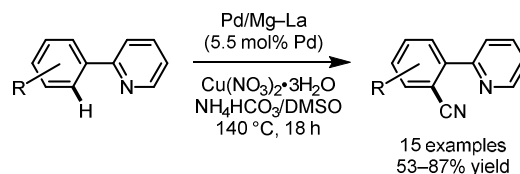
More recently, Kantam and co-workers have used a nanocrystalline magnesium oxide-stabilised Pd<sup>0</sup>NP catalyst (NAP-Mg-Pd<sup>0</sup>) for the synthesis of *N*-(2-pyridyl)indoles *via* a concise oxidative C–H bond functionalisation of *N*-aryl-2-aminopyridines with substituted alkynes (Scheme 19).<sup>94</sup> This catalyst was prepared by first calcining the magnesium oxide at 450 °C before treatment with Na<sub>2</sub>PdCl<sub>4</sub> to afford a NAP-Mg-PdCl<sub>4</sub> catalyst. This was then reduced with NaBH<sub>4</sub> to afford the supported Pd<sup>0</sup> catalyst, containing around 0.8 wt% Pd. It would appear that in this reaction the *N*-pyridyl motif is required as a directing group for the Pd catalyst to ensure high regioselectivity. During screening it was found that of several oxidants tested, only CuCl<sub>2</sub> proved efficacious, while other supported Pd<sup>0</sup> catalysts such as Pd/C provided no conversion.



**Scheme 19.** Synthesis of *N*-(2-pyridyl)indoles from *N*-aryl-2-aminopyridines and substituted alkynes using NAP-Mg-Pd<sup>0</sup> (Kantam *et al.*, 2015).<sup>94</sup>

This protocol was applied to a small range of aryl-aminopyridines and alkynes, demonstrating good tolerance for electron-donating and electron-withdrawing aryl substituents, while the least hindered C–H bond was selectively functionalised in all examples tested. Slight differences in conversion were observed with 3-substituted aromatics over the equivalent 4-substituted aromatics. The recyclability of this catalyst was investigated *via* recovery with centrifugation and found to be excellent, with consistent activity found after four cycles. Correspondingly, atomic absorption spectroscopy (AAS) demonstrated no leached Pd in the catalyst after being subjected to the reaction conditions, while TEM indicated no change in size or morphology.

A Pd<sup>II</sup>/Mg–La mixed oxide catalyst prepared by Kantam and co-workers has been demonstrated to effectively catalyse the cyanation of a range of arylpyridines, using a mixture of NH<sub>4</sub>HCO<sub>3</sub> and DMSO as the ‘CN’ source (Scheme 20).<sup>95</sup> This catalyst was prepared by formation of the Mg–La oxide from Mg(NO<sub>3</sub>)<sub>2</sub> and La(NO<sub>3</sub>)<sub>3</sub>, followed by impregnation with Pd(NO<sub>3</sub>)<sub>2</sub>. This process produced a material with Pd particle sizes of *ca.* 25 nm, containing 9.8 wt% Pd as measured by AAS. Relatively forcing conditions such as elevated temperatures and an external Cu oxidant were required however, in addition to the directing pyridyl motif, although the desired products were obtained in good to excellent yields, across a range of electron-donating and -withdrawing arylpyridines. It is also interesting to consider whether the nitrate anions are redox active in this chemistry.

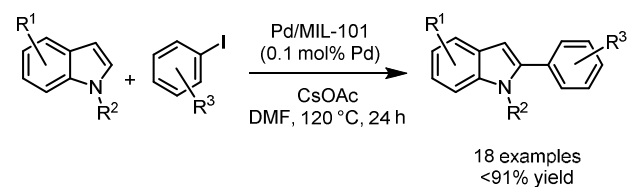


**Scheme 20.** Cyanation of arylpyridines using a mixed Mg–La supported Pd<sup>II</sup> oxide catalyst (Kantam *et al.*, 2015).<sup>95</sup>

The preparation of the catalyst from metal nitrates presents an interesting observation, as Pd nitrates (or systems containing both Pd species and nitrate sources) are known to act as strong oxidants in their own right, particularly when used with directing substrates such as arylpyridines, piperidines or quinolines.<sup>96–98</sup> Additionally, Pd(NO<sub>3</sub>)<sub>2</sub> is known to undergo facile hydrolysis to Pd(OH)<sub>2</sub>, which can adversely affect the templating process used to synthesise other Pd-metal nanocatalysts.<sup>99</sup> AAS measurements of the post-reaction mixture indicated around 10% Pd leaching from the catalyst after each reaction cycle, although recyclability of the catalyst over four cycles shown no appreciable decrease in conversion. It was therefore proposed by the authors that leached Pd species are the relevant catalytic species in this reaction; removal of the catalyst from the reaction mixture after 3 h did not affect conversion, hinting at the involvement of such leached Pd species.

### Metal–organic frameworks

In addition to those metal–metal catalysts detailed above, supported Pd nanoparticulate catalysts incorporating the catalytic Pd source within metal–organic frameworks (MOFs) have also been reported.<sup>100, 101</sup> Cao and co-workers described the direct C2-arylation of indoles with aryl halides using the Cr-containing MOF MIL-101 impregnated with PdNPs (Scheme 21).<sup>102</sup> The resulting Pd/MIL-101 material demonstrated two different cavity sizes within its mesoporous structure, 2.9 nm and 3.4 nm, which contained PdNPs with an average diameter of 2.6 ± 0.5 nm. These PdNPs were confirmed as Pd<sup>0</sup> by XPS and were present at an approximately 0.5 wt% loading.

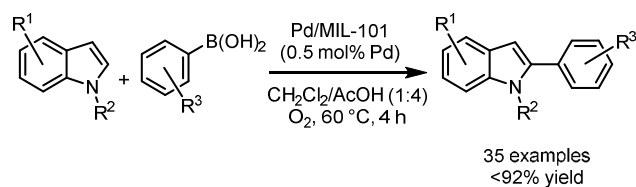


**Scheme 21.** Direct C2-arylation of indoles with aryl iodides using a Cr MOF-supported PdNP catalyst (Cao *et al.*, 2011).<sup>102</sup>

Good to excellent yields were observed for a range of electron-donating and electron-withdrawing aryl iodides in the *meta*- and *para*- positions; aryl bromides and chlorides proved much less effective however, requiring increased temperatures and reaction times. The *N*-substituent on the indole proved critical; electron-donating *N*-Me and *N*-*n*Bu indoles generally gave high yields while free *N*-H or electron-withdrawing *N*-Ac indoles resulted in severely decreased yields. Finally, a small electronic effect was seen for substituents on the indole ring, with electron-rich indoles providing higher yields, mirroring the effect of the *N* protecting group.

Post-workup analysis using inductively coupled plasma atomic emission spectroscopy (ICP-AES) showed the presence of only 0.4 ppm Pd, indicating little Pd leaching under the reaction conditions, while no leached Cr was observed. Correspondingly this catalyst demonstrated excellent recyclability, with a decrease in yield of only 4% after five uses; TEM analysis after each use indicated little or no PdNP growth or distortion. The hot filtration test also showed no further conversion to product after filtration of the catalyst.

To address the high temperatures and long reaction times needed for this transformation, aryl boronic acids were used in place of aryl halides for the direct C2-arylation of indoles catalysed by Pd/MIL-101 in later work from the same group (**Scheme 22**).<sup>103</sup>



**Scheme 22.** Direct C2-arylation of indoles with aryl boronic acids using a Cr MOF-supported PdNP catalyst (Cao *et al.*, 2013).<sup>103</sup>

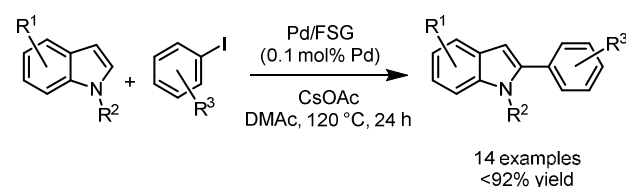
To facilitate high conversion, it was found that acidic conditions and an oxidising atmosphere were required in this instance, allowing for significant reductions in both reaction time and temperature. Interestingly, greater quantities of the C3-arylated and C2,3-diarylated byproducts were observed in this system when compared to the aryl halide protocol. A broad range of aryl boronic acids were tolerated under these conditions, as were *N*-Me and free *N*-H indoles. *N*-Ac and *N*-Boc indoles were also effective in several cases, but proved problematic when coupled with electron-deficient indole rings. Addition of the radical initiator TEMPO along with KF

circumvented this limitation and allowed access to the desired products in high yields.

As with the previous methodology, application of the hot filtration test indicated that the catalytically competent species was likely heterogeneous in nature, while ICP-AES analysis demonstrated only 0.9 ppm Pd in the post-reaction mixture. Catalyst recyclability was also very good, with a decrease in yield of only 3% after five catalysts uses; powder X-ray diffraction (XRD) indicated that the catalyst had retained its crystallinity even after several recovery/reuse cycles.

### Silicon-based frameworks

Another reasonably well-explored method of supporting PdNPs is through the use of modified silicas. One such early example by Cai and co-workers utilised fluorosilica gel to support PdNPs which had been tagged with a perfluoroalkane; this enabled stabilisation by exploiting fluorosilica–fluorosilica interactions between the tagged PdNPs and the silica gel support.<sup>104</sup> By this method, PdNPs of around 2 nm were obtained. This catalyst (here defined as Pd/FSG) was evaluated in the direct C2-arylation of a range of indoles with aryl halides (**Scheme 23**).

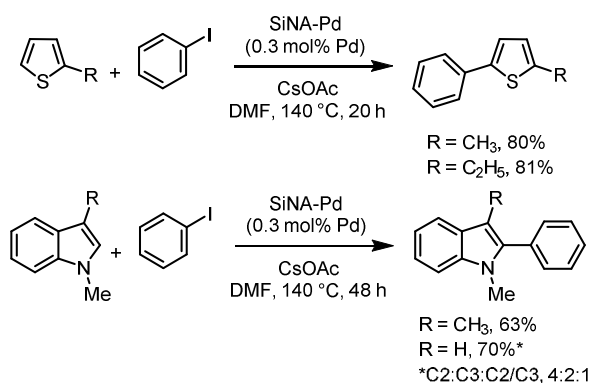


**Scheme 23.** Direct C2-arylation of indoles with aryl iodides using a fluorosilica gel-supported PdNP catalyst (Cai *et al.*, 2011).<sup>104</sup>

As with previous examples highlighted above, *N*-Me indoles proved the most effective, with free *N*-H indoles giving reduced yields and *N*-Ac indoles giving none of the desired product; electron-deficient indole rings also resulted in lower yields. Aryl iodides were found to give higher yields of the desired products than aryl bromides, although a range of aryl iodides containing electron-withdrawing or electron-donating groups were tolerated and as expected, *ortho*-substituted aryl iodides reacted more slowly than *para*-substituted examples. A simple recycling experiment demonstrated excellent catalyst recyclability after five runs (a decrease in yield of 6% was seen), while the hot filtration test and ICP analysis indicated that a heterogeneous catalytic manifold was likely in operation.

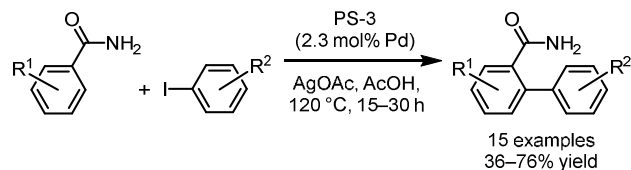
Uozumi and co-workers have developed a silicon nanowire hybrid Pd catalyst, SiNA-Pd, obtained by reduction of K<sub>2</sub>PdCl<sub>4</sub> onto a prepared Si nanowire surface.<sup>105</sup> This produced PdNPs of ca. 5–10 nm diameter, which demonstrated high activity in the direct arylation of a small number of thiophenes and indoles (**Scheme 24**). No investigation of catalyst recycling or mechanistic determination on this system was performed, although good recyclability was observed when using this catalyst for a series of Mizoroki–Heck couplings of aryl halides

with terminal alkenes. The typical hot filtration and ICP-AES tests indicated a probable heterogeneous manifold.



**Scheme 24.** Direct arylation of thiophenes and indoles with iodobenzene using a silicon nanowire-supported PdNP catalyst (Uozumi *et al.*, 2014).<sup>105</sup>

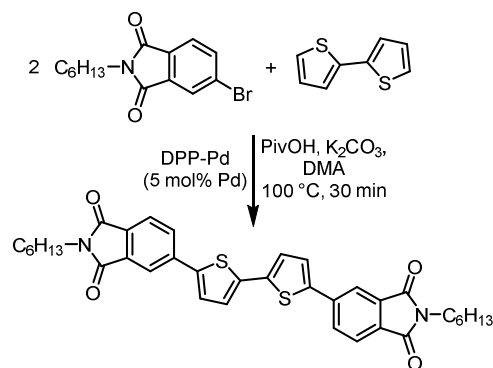
A calcined mesoporous silica has been used by Srinivasu and co-workers to support highly dispersed PdNPs, obtained through loading with Pd(OAc)<sub>2</sub>.<sup>106</sup> The PS-3 catalyst contains particles of approximately 7–8 nm which display well resolved (111), (200) and (220) planes, indicating face-centered cubic structures. This demonstrated good activity in the *ortho*-arylation of benzamides with aryl iodides (**Scheme 25**). A broad range of aryl iodides were tolerated, although electron-deficient substrates gave noticeably lower yields. Similarly, amides containing electron-donating aromatic groups provided higher yields than electron-withdrawing examples.



**Scheme 25.** Direct *ortho*-arylation of benzamides with aryl iodides using a mesoporous silica PdNP catalyst (Srinivasu *et al.*, 2014).<sup>106</sup>

Catalyst recycling in this system was very good, with equivalent activity and selectivity obtained after five re-uses. Additionally, no leached Pd was detected in the post-reaction mixture by ICP whilst wide-angle XRD performed on the recovered catalyst demonstrated metallic Pd at similar binding energies to the fresh PS-3 catalyst.

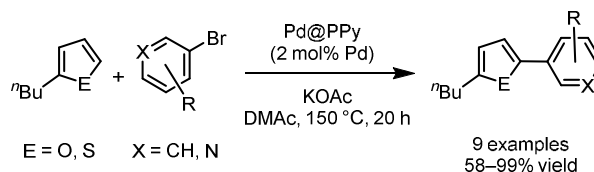
Welch and co-workers have explored the activity of a commercially available SiliaCat<sup>®</sup> Pd-containing catalyst, DPP-Pd, in a direct sp<sup>2</sup>–sp<sup>2</sup> coupling reaction to form a phthalimide-thiophene-based semiconductor (**Scheme 26**).<sup>107</sup> In this example, the Pd catalyst is tethered to a silica support *via* an alkyl phosphine ligand.



**Scheme 26.** Formation of a phthalimide-thiophene-based semiconductor *via* a silica-supported Pd-catalysed direct coupling (Welch *et al.*, 2015).<sup>107</sup>

### Carbon-based frameworks

Several examples of Pd nanocatalysts supported on organic frameworks, in various forms, have been demonstrated to be effective in C–H bond functionalisation processes. Hierso and co-workers have prepared a palladium–polypyrrole catalyst, Pd@PPy, which contains nanoparticulate Pd of approximately 2 nm stabilised within spherical polypyrrole structures.<sup>108</sup> These were easily prepared by the reduction of [Pd(NH<sub>3</sub>)<sub>4</sub>Cl<sub>2</sub>] in the presence of polypyrrole, affording a material notable for its unusually high nanoparticulate Pd loading (35 wt%). Other key features of these nanocatalysts are their highly colloidal nature, as indicated by SEM and TEM images, as well as their high ratio of surface-bound to bulk Pd, as indicated by XPS analysis. This catalyst was shown to be effective in the direct C<sub>2</sub>-arylation of furans and thiophenes with bromoarenes (**Scheme 27**).

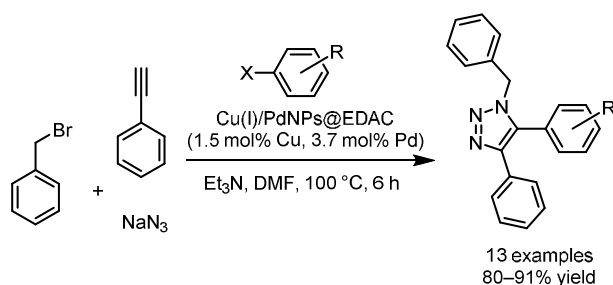


**Scheme 27.** Direct C<sub>2</sub>-arylation of furans and thiophenes with bromoarenes using a Pd-polypyrrole nanocatalysts (Hierso *et al.*, 2011).<sup>108</sup>

Electron-rich and electron-poor aryl bromides were well tolerated under these conditions and 2 examples using bromoquinolines provided the desired products in high conversion without catalyst poisoning. Steric effects were however shown to be critical, with no conversion seen when using the hindered 2,4,6-trimethylbromobenzene. Catalyst recyclability was investigated and found to give inconsistent results; coupling of 2-*n*-butylfuran with 4-bromobenzonitrile could be repeated at similar conversions using the recycled catalyst whilst the equivalent coupling with 4-bromoacetophenone failed upon catalyst reuse. Subsequent investigation using TEM established a growth of the PdNP particle sizes from 4 to 7 nm under the reaction conditions, which is likely the cause of the loss of catalytic activity, smaller

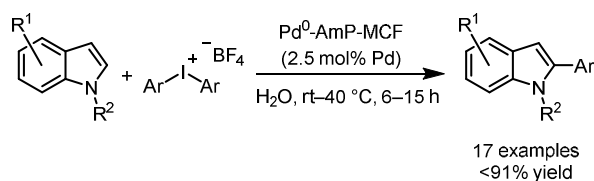
particles *in general* providing greater activity due to their higher proportion of surface defect sites (*vide supra*). Interestingly SEM images indicated no distortion of the spherical polypyrrole support, implying that the majority of the PdNPs dispersed throughout the structure are catalytically relevant (and correspondingly their growth occurs concomitantly).

Ethylenediamine functionalised cellulose (EDAC) has been used to support Cu<sup>I</sup> and 5–10 nm PdNPs by Shaabani and co-workers, with the resulting Cu<sup>I</sup>/PdNPs@EDAC catalyst demonstrating activity in a 1,3-dipolar cycloaddition/direct arylation sequence (**Scheme 28**).<sup>109</sup> This procedure tolerated a range of aryl halides containing electron-donating and electron-withdrawing functionality, with the catalyst demonstrating excellent recyclability over four recovery/reuse cycles.



**Scheme 28.** Synthesis of trisubstituted triazoles using a cellulose-supported Cu<sup>I</sup>/PdNP catalyst (Shaabani *et al.*, 2014).<sup>109</sup>

A catalyst comprising PdNPs supported on an amino-functionalised mesocellular foam (Pd<sup>0</sup>-AmP-MCF) prepared by the Bäckvall group<sup>110</sup> has been utilised by Olofsson and co-workers in the direct C2-arylation of indoles with aryl iodonium salts (**Scheme 29**).<sup>111</sup> This support contains many mesoporous cavities enabling the stabilisation of well-dispersed 2–3 nm PdNPs; XPS analysis revealed the presence of both Pd<sup>0</sup> and Pd<sup>II</sup> particles in an approximately 3:1 ratio. The analogous non-reduced Pd<sup>II</sup>-AmP-MCF did however display decreased reactivity, implying that the Pd<sup>0</sup> species are more competent catalysts in this system.



**Scheme 29.** Direct C2-arylation of indoles with aryl iodonium salts using an amino-functionalised mesocellular foam (Olofsson *et al.*, 2014).<sup>111</sup>

A series of electron-donating, electron-withdrawing and sterically hindered aryl iodonium salts were demonstrated to be effective under the reaction conditions. Some modification of the electronic nature of the indole ring also allowed good conversion to the desired products, notably free *N-H* indoles were tolerated in some cases. Unfortunately however the use of differentially substituted diaryliodonium salts containing the

non-transferable 2,4,6-trimethylphenyl (mesityl) or 2,4,6-triisopropylphenyl (TRIP) dummy groups were less active in this system, limiting their use for the installation of more complex functionality. The recyclability of this catalyst was also investigated, albeit with significantly reduced yields, with losses of 33% conversion observed in the third cycle. ICP-OES analysis however indicated very little leached Pd in the post-reaction mixture (0.6 ppm), hence dispersion of Pd within the mesoporous foam away from the active nanoclusters, into less active aminopropyl groups was suggested as an explanation for the loss of activity. This also may provide an explanation as to why the Pd<sup>II</sup>-AmP-MCF demonstrated lower activity under these reaction conditions.

A family of macrocyclic cucurbituril frameworks have been used to support PdNPs by Cao and co-workers, the resulting catalysts being demonstrated to effectively catalyse the direct arylation of a range of fluoroarenes with aryl halides.<sup>112</sup> Of the four ring sizes tested (5–8), CB[6]-PdNPs (*ca.* 3.8 nm) afforded the highest conversion to the desired products (**Scheme 30**). This is rationalised on the basis of the distinct structures obtained, with TEM indicating that while the PdNPs are uniformly distributed throughout each catalyst, the specific morphology of each differs according to the specific macrocycle used. The shape of the CB[6]-PdNPs appear to be more regular, with less particle clustering than in the CB[5], CB[7] or CB[8] examples, resulting in greater exposed surface areas for the CB[6]-PdNPs. Additionally, <sup>1</sup>H NMR spectroscopic studies indicated stronger interactions between the substrates and CB[5], CB[7] and CB[8], while CB[6] appears to act purely as a PdNP stabilising agent with no substrate/CB[6] interaction observed.



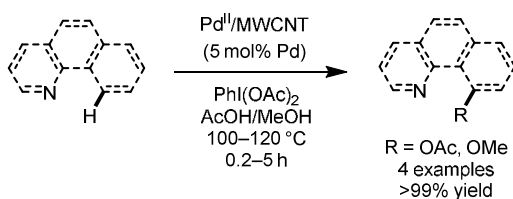
**Scheme 30.** Direct arylation of fluoroarenes with aryl halides using a cucurbit[6]uril PdNP catalyst (Cao *et al.*, 2015).<sup>112</sup>

This protocol demonstrated good tolerance for electron-donating and electron-withdrawing aryl halides, providing moderate to high conversions for a range of challenging tri-, tetra- and penta-fluorinated aromatics, albeit with high temperatures and long reaction times. The standard Hg drop and hot filtration tests inhibited the reaction, providing good indications of heterogeneity in this system. This was further supported by high catalyst recyclability, with around 90% of reactivity retained in the fifth cycle; HR-TEM indicated that while the particle size increased during the reaction (to around 10 nm), critically the defect sites on the surface of the PdNPs were well-maintained.

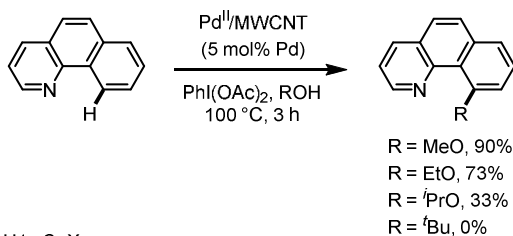
Ellis and co-workers have probed the reaction of Pd<sup>II</sup>NPs supported on multiwalled carbon nanotubes (Pd<sup>II</sup>/MWCNT) in several chelation-assisted direct sp<sup>2</sup> C–H bond functionalisation reactions (**Scheme 31**).<sup>113</sup> Intriguingly, in many of these examples reactivity distinct from that seen

when using the more commonly employed Pd(OAc)<sub>2</sub> was realised; increased activity but reduced substrate tolerance was seen in some acetoxylation reactions (**Scheme 31a**), reduced yields obtained in some alkoxylation reactions (**Scheme 31b**) and significantly increased rates observed in halogenations using *N*-bromo- or *N*-chlorosuccinimide (**Scheme 31c**). Specifically, catalyst recycling in the methoxylation of 8-methylquinolone was superb with minimal loss of activity after 16 recovery/reuse cycles (8% decrease); ICP-MS analysis of the post-reaction mixture correspondingly demonstrated almost no leaching with <250 ppb Pd found, while the hot filtration test was seen to prevent further conversion.

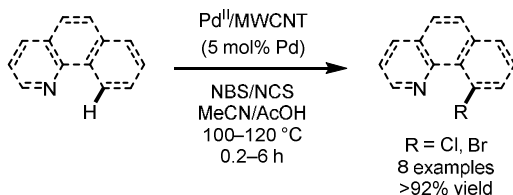
## a) C–H to C–O



## b) C–H to C–OR

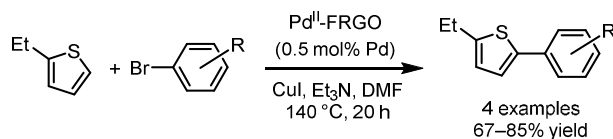


## c) C–H to C–X



**Scheme 31.** Direct C–H bond functionalisation of *N*-chelating substrates under oxidising conditions using a carbon nanotube supported Pd<sup>II</sup>NP catalyst (Ellis *et al.*, 2015).<sup>113</sup>

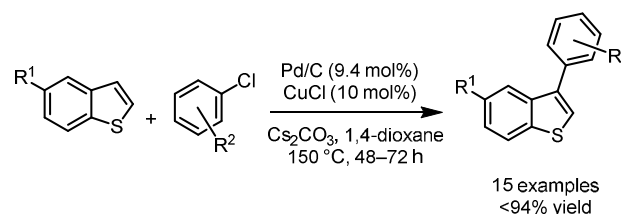
Xi and co-workers have prepared a Pd nanocatalyst supported on functional graphene oxide (Pd<sup>II</sup>-FRGO), obtained by doping of a pre-prepared graphene oxide with PdCl<sub>2</sub> in DMF at room temperature, producing particles of *ca.* 6 nm with the bulk solid containing approximately 4.8 wt% Pd. This catalyst was shown to be effective in Pd-catalysed cross-coupling processes such as the Suzuki–Miyaura and Mizoroki–Heck reactions, in addition to the direct arylation of 2-ethylthiophene (**Scheme 32**).<sup>114</sup>



**Scheme 32.** Direct arylation of 2-ethylthiophene with aryl bromides using a functionalised graphene oxide Pd nanocatalyst (Xi *et al.*, 2015).<sup>114</sup>

## Pd/C for direct C–H bond functionalisation

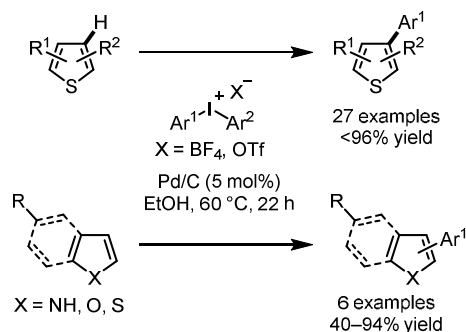
Despite its widespread use as a heterogeneous hydrogenation catalyst, Pd/C has only recently been examined for other Pd-mediated catalysis, usually in cross-coupling reactions.<sup>11–14</sup> Glorius and co-workers are particularly notable for their continuing development of C–H bond functionalisation reactions using this catalyst. The first such example described the direct arylation of benzo[*b*]thiophenes with aryl chlorides, affording C3-arylated products with extremely high selectivity (**Scheme 33**).<sup>115</sup> Despite the excellent C3-selectivity, high temperatures and long reaction times were required to provide synthetically useful yields, although the use of typically less activated aryl chlorides over aryl iodides or bromides is of significant benefit. A broad range of aryl chlorides were tolerated, including those with *ortho*-substituents while CuCl was found to be necessary to ensure higher yields, with Lewis acid activation of the benzo[*b*]thiophene its proposed role.



**Scheme 33.** Direct C3-arylation of benzo[*b*]thiophenes with aryl chlorides using Pd/C (Glorius *et al.*, 2013).<sup>115</sup>

As with more recent work from this group, the hot filtration test showed no further conversion to product after filtration, the three-phase test demonstrated that no *active* homogeneous palladium species were formed under the reaction conditions and the reaction was seen to be dependent on rapid stirring rates. TXRF spectroscopy demonstrated <4 ppm Pd in the post-reaction mixture. Interestingly the source of Pd/C used for this reaction had a pronounced effect on yield, with variation of up to 59% between suppliers observed. This would suggest that the nature of the support or Pd morphology (*vide supra*) is critical to reactivity; correspondingly for other catalytic systems material from different suppliers may prove more efficacious. Some nominally homogeneous Pd catalysts proved able to catalyse this reaction, although fascinatingly these gave a complete switch in selectivity, with exclusively C2-arylated products being obtained.

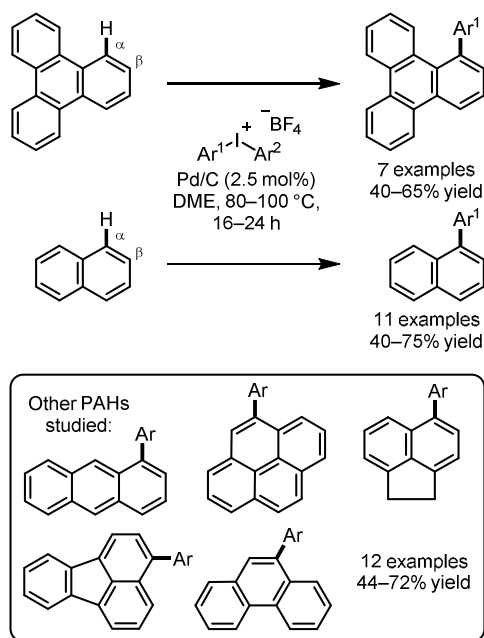
Subsequent development in the arylation of thiophenes, benzo[*b*]thiophenes and other related heterocycles replaced the aryl chlorides with arylidonium salts, which allowed for much milder conditions to be used (**Scheme 34**).<sup>116</sup> This new protocol also demonstrated wide-ranging applicability with regard to substituents on both the thiophene and arylating agent, with differentially substituted arylidonium salts containing the TRIP dummy group utilised to vary the installed arene. A brief substrate screen also indicated that indoles, furans and benzofurans were reactive under these conditions.



**Scheme 34.** Direct arylation of thiophenes and related heterocycles with aryliodonium salts using Pd/C (Glorius *et al.*, 2014).<sup>116</sup>

The same heterogeneity tests as before were performed, again indicating a heterogeneous catalytic manifold despite the strongly oxidising conditions. Catalyst recycling was however poor, with a significant decrease (41%) in yield observed after three cycles. Pd(OAc)<sub>2</sub> was also shown to catalyse this reaction, albeit with lower efficiency than Pd/C. Intriguingly when the conditions employing Pd(OAc)<sub>2</sub> were subjected to the three-phase test, they indicated possible homogeneous behaviour, leading the authors to suggest that Pd(OAc)<sub>2</sub> could be acting as a reservoir for heterogeneous Pd species *i.e.* PdNPs (as highlighted *vide supra*).

More recently, a modification of this protocol was applied to the direct arylation of triphenylene, naphthalene and other related polyaromatic hydrocarbons (PAHs) (**Scheme 35**).<sup>117</sup> Surprisingly, arylation typically occurred at the most hindered position in these systems, with high  $\alpha:\beta$  selectivity observed in many cases.



**Scheme 35.** Direct arylation of triphenylene, naphthalene and related PAHs with aryliodonium salts using Pd/C (Glorius *et al.*, 2015).<sup>117</sup>

A series of electron-donating and electron-withdrawing substituents were also demonstrated to give good yields for triphenylene and naphthalene. Attempts to functionalise substituted naphthalenes however met with limited or no success. In all cases side-products were found which resulted from polyarylation of the PAH; suppressing this is, to quote the authors, “an unmet challenge”. Interestingly, Pd/Al<sub>2</sub>O<sub>3</sub> also proved an effective catalyst, although it gave reduced yields when compared to Pd/C.

Tests for heterogeneity all indicated the same results as with previous methods using Pd/C (*vide supra*), although the authors note that the high temperatures and oxidative conditions used mean it is probable that Pd leaching does occur in this case. The tests performed would seem to indicate that homogeneous Pd was not active in this system, but that does not preclude the possibility of heterogeneous leached Pd (*i.e.* PdNPs) being the active catalyst. The reaction was found to be first-order for Pd, with decreasing induction periods at higher Pd loadings, which is indicative of formation of the active catalyst being the rate-determining step. The reaction was also found to be zeroth-order for naphthalene, with an unusual inverse kinetic isotope effect (KIE) of 0.54, while reactivity was inhibited by addition of TEMPO, BHT and BQ. These mechanistic studies led the authors to conclude that insoluble PdNPs leached into solution from the Pd/C support are the catalytically relevant species in a Pd<sup>0</sup>/Pd<sup>II</sup> manifold, involving a key carbon-centred radical intermediate formed by single electron reduction of the aryliodonium salt.

## Conclusions

The case for the involvement of mononuclear (quasi)homogeneous and multinuclear (quasi)heterogeneous catalysis has been made in this article. Examination of the discoveries made in the field of traditional Pd-catalysed cross-coupling with regard to ultra-low catalyst loadings (ppm to ppb), inverse rate correlations and the ability of common Pd precursors to act as catalyst reservoirs, creates a solid foundation upon which to study C–H bond functionalisation processes. An understanding of these complex effects will allow future research to make more effective use of precious Pd, both through reductions in catalyst loading and the recyclability that heterogeneous catalysis can offer.

Discoveries in this area thus far fall into two classifications; groups who wish to develop heterogeneous Pd catalysts then design a system which is exemplified on typically simple substrates, or researchers in the process of creating a desired structural motif encounter heterogeneous behaviour in one of their catalytic transformations and perform tests to evaluate this phenomenon. Combining intelligent heterogeneous catalyst design with the ability to access desirable chemical structures is of paramount importance in the development of this field. The advantages of this approach would be exemplified further if such catalysts could be demonstrated to effect transformations impossible or at least highly challenging for more common homogenous Pd precursors. Pleasingly, some promising progress has been made, with several

heterogeneous catalysts demonstrating markedly different reactivity to common Pd precursors, such as increased activity or even differing regioselective outcomes.

Finally, it is highly likely that examples of heterogeneous behaviour has gone unnoticed due to the inherent difficulties in probing it, *i.e.* the tools needed to study processes are not yet universally adopted by synthetic chemists (*e.g.* TEM, XAS, XPS analysis). It is however apparent that new advanced techniques and methods are needed for the characterisation of (quasi)heterogeneous catalysts generated from homogenous precursor catalysts. This insight has the potential to inform the design of future catalytic processes.†

## Acknowledgements

We are grateful for funding from the Innovative Medicines Initiative Joint Undertaking under grant agreement n°115360 (Chem21 project), resources of which are composed of financial contribution from the European Union's Seventh Framework Programme (FP7/2007-2013) and EFPIA companies' in kind contribution. We thank the EPSRC and Royal Society for past funding supporting our efforts to examine the role played by Pd nanoparticles in cross-coupling processes.

## Notes

† During the final stages of the preparation of our feature article we noticed the publication of a complementary review article on this topic by McGlacken.<sup>118</sup>

## References

1. L. Ackermann, R. Vicente and A. R. Kapdi, *Angew. Chem. Int. Ed.*, 2009, **48**, 9792.
2. J. Yamaguchi, A. D. Yamaguchi and K. Itami, *Angew. Chem. Int. Ed.*, 2012, **51**, 8960.
3. A. J. Hunt, T. J. Farmer and J. H. Clark, in *Element Recovery and Sustainability*, ed. A. J. Hunt, RSC Publishing, Cambridge, UK, 2013, ch. 1, p. 1.
4. G. Cahiez, C. Duplais and J. Buendia, *Chem. Rev.*, 2009, **109**, 1434.
5. R. I. Khusnutdinov, A. R. Bayguzina and U. M. Dzhemilev, *Russ. J. Org. Chem.*, 2012, **48**, 309.
6. A. Correa, O. Garcia Mancheno and C. Bolm, *Chem. Soc. Rev.*, 2008, **37**, 1108.
7. I. Bauer and H.-J. Knölker, *Chem. Rev.*, 2015, **115**, 3170.
8. G. Cahiez and A. Moyeux, *Chem. Rev.*, 2010, **110**, 1435.
9. K. Gao and N. Yoshikai, *Acc. Chem. Res.*, 2014, **47**, 1208.
10. L. Ackermann, *J. Org. Chem.*, 2014, **79**, 8948.
11. Á. Molnár, *Chem. Rev.*, 2011, **111**, 2251.
12. A. Balanta, C. Godard and C. Claver, *Chem. Soc. Rev.*, 2011, **40**, 4973.
13. H.-U. Blaser, A. Indolese, A. Schnyder, H. Steiner and M. Studer, *J. Mol. Catal. A: Chem.*, 2001, **173**, 3.
14. Yin and J. Liebscher, *Chem. Rev.*, 2007, **107**, 133.
15. D. L. Davies, S. M. A. Donald and S. A. Macgregor, *J. Am. Chem. Soc.*, 2005, **127**, 13754.
16. M. Lafrance, C. N. Rowley, T. K. Woo and K. Fagnou, *J. Am. Chem. Soc.*, 2006, **128**, 8754.
17. Y. Boutadla, D. L. Davies, S. A. Macgregor and A. I. Poblador-Bahamonde, *Dalton Trans.*, 2009, 5820.
18. X. Chen, K. M. Engle, D.-H. Wang and J.-Q. Yu, *Angew. Chem. Int. Ed.*, 2009, **48**, 5094.
19. O. Daugulis, H.-Q. Do and D. Shabashov, *Acc. Chem. Res.*, 2009, **42**, 1074.
20. J. M. Racowski, A. R. Dick and M. S. Sanford, *J. Am. Chem. Soc.*, 2009, **131**, 10974.
21. D. C. Powers, M. A. L. Geibel, J. E. M. N. Klein and T. Ritter, *J. Am. Chem. Soc.*, 2009, **131**, 17050.
22. D. C. Powers and T. Ritter, *Nat Chem*, 2009, **1**, 302.
23. P. Sehnal, R. J. K. Taylor and I. J. S. Fairlamb, *Chem. Rev.*, 2010, **110**, 824.
24. T. W. Lyons and M. S. Sanford, *Chem. Rev.*, 2010, **110**, 1147.
25. L. Ackermann, *Chem. Rev.*, 2011, **111**, 1315.
26. D. C. Powers, E. Lee, A. Ariafard, M. S. Sanford, B. F. Yates, A. J. Canty and T. Ritter, *J. Am. Chem. Soc.*, 2012, **134**, 12002.
27. K. M. Engle, T.-S. Mei, M. Wasa and J.-Q. Yu, *Acc. Chem. Res.*, 2012, **45**, 788.
28. P. Ricci, K. Krämer, X. C. Cambeiro and I. Larrosa, *J. Am. Chem. Soc.*, 2013, **135**, 13258.
29. A. N. Vedernikov, in *C-H and C-X Bond Functionalization: Transition Metal Mediation*, ed. X. Ribas, RSC Publishing, Cambridge, UK, 2013, ch. 4, p. 108.
30. J. R. Khusnutdinova and L. M. Mirica, in *C-H and C-X Bond Functionalization: Transition Metal Mediation*, ed. X. Ribas, RSC Publishing, Cambridge, UK, 2013, ch. 5, p. 122.
31. J. J. Topczewski and M. S. Sanford, *Chem. Sci.*, 2015, **6**, 70.
32. H. Ramezani-Dakhel, P. A. Mirau, R. R. Naik, M. R. Knecht and H. Heinz, *Phys. Chem. Chem. Phys.*, 2013, **15**, 5488.
33. J. A. Widegren and R. G. Finke, *J. Mol. Catal. A: Chem.*, 2003, **198**, 317.
34. R. H. Crabtree, *Chem. Rev.*, 2012, **112**, 1536.
35. I. J. S. Fairlamb and A. F. Lee, in *C-H and C-X Bond Functionalization: Transition Metal Mediation*, ed. X. Ribas, RSC Publishing, Cambridge, UK, 2013, ch. 3, p. 72.
36. R. H. Crabtree, *Chem. Rev.*, 2015, **115**, 127.
37. A. H. M. de Vries, J. M. C. A. Mulders, J. H. M. Mommers, H. J. W. Henderickx and J. G. de Vries, *Org. Lett.*, 2003, **5**, 3285.
38. I. J. S. Fairlamb, A. R. Kapdi, A. F. Lee, G. Sanchez, G. Lopez, J. L. Serrano, L. Garcia, J. Perez and E. Perez, *Dalton Trans.*, 2004, 3970.
39. N. E. Leadbeater and M. Marco, *Org. Lett.*, 2002, **4**, 2973.
40. C. Deraedt and D. Astruc, *Acc. Chem. Res.*, 2014, **47**, 494.
41. (a) F. Zhao, B. M. Bhanage, M. Shirai and M. Arai, *Chem. Eur. J.*, 2000, **6**, 843. A very recent paper reports the use of a laponite clay in Mizoroki-Heck type reactions, see: (b) J. I. García, F. Invernizzi, A. Leal, A. Martínez and J.A. Mayoral, *RSC Advances*, 2015, **5**, 59983.
42. J. B. Brazier, B. N. Nguyen, L. A. Adrio, E. M. Barreiro, W. P. Leong, M. A. Newton, S. J. A. Figueroa, K. Hellgardt and K. K. M. Hii, *Catal. Today*, 2014, **229**, 95.
43. C. C. Cassol, A. P. Umpierre, G. Machado, S. I. Wolke and J. Dupont, *J. Am. Chem. Soc.*, 2005, **127**, 3298.

## ARTICLE

## Journal Name

44. M. B. Thathagar, J. E. ten Elshof and G. Rothenberg, *Angew. Chem. Int. Ed.*, 2006, **45**, 2886.
45. A. V. Gaikwad and G. Rothenberg, *Phys. Chem. Chem. Phys.*, 2006, **8**, 3669.
46. S. Reimann, J. Stoetzel, R. Frahm, W. Kleist, J.-D. Grunwaldt and A. Baiker, *J. Am. Chem. Soc.*, 2011, **133**, 3921.
47. P. J. Ellis, I. J. S. Fairlamb, S. F. J. Hackett, K. Wilson and A. F. Lee, *Angew. Chem. Int. Ed.*, 2010, **49**, 1820.
48. A. F. Lee, P. J. Ellis, I. J. S. Fairlamb and K. Wilson, *Dalton Trans.*, 2010, **39**, 10473.
49. T. Teranishi and M. Miyake, *Chem. Mater.*, 1998, **10**, 594.
50. J. Le Bars, U. Specht, J. S. Bradley and D. G. Blackmond, *Langmuir*, 1999, **15**, 7621.
51. G. Collins, M. Schmidt, C. O'Dwyer, J. D. Holmes and G. P. McGlacken, *Angew. Chem. Int. Ed.*, 2014, **53**, 4142.
52. G. Collins, M. Schmidt, G. P. McGlacken, C. O'Dwyer and J. D. Holmes, *J. Phys. Chem. C*, 2014, **118**, 6522.
53. G. Collins, M. Schmidt, C. O'Dwyer, G. McGlacken and J. D. Holmes, *ACS Catalysis*, 2014, **4**, 3105.
54. T. E. Storr, A. G. Firth, K. Wilson, K. Darley, C. G. Baumann and I. J. S. Fairlamb, *Tetrahedron*, 2008, **64**, 6125.
55. T. E. Storr, C. G. Baumann, R. J. Thatcher, S. De Ornellas, A. C. Whitwood and I. J. S. Fairlamb, *J. Org. Chem.*, 2009, **74**, 5810.
56. M. Hyotanishi, Y. Isomura, H. Yamamoto, H. Kawasaki and Y. Obora, *Chem. Commun.*, 2011, **47**, 5750.
57. H. Yano, Y. Nakajima and Y. Obora, *J. Organomet. Chem.*, 2013, **745–746**, 258.
58. M. Chiba, M. N. Thanh, Y. Hasegawa, Y. Obora, H. Kawasaki and T. Yonezawa, *J. Mater. Chem. C*, 2015, **3**, 514.
59. S. Sahnoun, S. Messaoudi, J.-F. Peyrat, J.-D. Brion and M. Alami, *Tetrahedron Lett.*, 2008, **49**, 7279.
60. S. Sahnoun, S. Messaoudi, J.-D. Brion and M. Alami, *Org. Biomol. Chem.*, 2009, **7**, 4271.
61. M. Parisien, D. Valette and K. Fagnou, *J. Org. Chem.*, 2005, **70**, 7578.
62. L. A. Adrio, B. N. Nguyen, G. Guilera, A. G. Livingston and K. K. Hii, *Catal. Sci. Tech.*, 2012, **2**, 316.
63. L. Djakovitch, M. Wagner, C. G. Hartung, M. Beller and K. Koehler, *J. Mol. Catal. A: Chem.*, 2004, **219**, 121.
64. L. Zhang, Z. Li, Y. Zhang, M. Chin Paau, Q. Hu, X. Gong, S. Shuang, C. Dong, X. Peng and M. M. F. Choi, *Talanta*, 2015, **131**, 632.
65. E. Raluy, I. Favier, A. M. Lopez-Vinasco, C. Pradel, E. Martin, D. Madec, E. Teuma and M. Gomez, *Phys. Chem. Chem. Phys.*, 2011, **13**, 13579.
66. L. Adak, S. Bhadra and B. C. Ranu, *Tetrahedron Lett.*, 2010, **51**, 3811.
67. D. Saha, L. Adak and B. C. Ranu, *Tetrahedron Lett.*, 2010, **51**, 5624.
68. P. Ehlers, A. Petrosyan, J. Baumgard, S. Jopp, N. Steinfeld, T. V. Ghochikyan, A. S. Saghyan, C. Fischer and P. Langer, *ChemCatChem*, 2013, **5**, 2504.
69. L. Nassar-Hardy, C. Deraedt, E. Fouquet and F.-X. Felpin, *Eur. J. Org. Chem.*, 2011, **2011**, 4616.
70. S. S. Zaleskiy and V. P. Ananikov, *Organometallics*, 2012, **31**, 2302.
71. E. O. Pentsak, A. S. Kashin, M. V. Polynski, K. O. Kvashnina, P. Glatzel and V. P. Ananikov, *Chem. Sci.*, 2015, **6**, 3302.
72. R. B. Bedford, J. G. Bowen, R. B. Davidson, M. F. Haddow, A. E. Seymour-Julen, H. A. Sparkes and R. L. Webster, *Angew. Chem. Int. Ed.*, 2015, **54**, 6591.
73. C. G. Baumann, S. De Ornellas, J. P. Reeds, T. E. Storr, T. J. Williams and I. J. S. Fairlamb, *Tetrahedron*, 2014, **70**, 6174.
74. T. J. Williams and I. J. S. Fairlamb, *Tetrahedron Lett.*, 2013, **54**, 2906.
75. N. R. Deprez, D. Kalyani, A. Krause and M. S. Sanford, *J. Am. Chem. Soc.*, 2006, **128**, 4972.
76. T. J. Williams, A. J. Reay, A. C. Whitwood and I. J. S. Fairlamb, *Chem. Commun.*, 2014, **50**, 3052.
77. A. J. Reay, T. J. Williams and I. J. S. Fairlamb, *Org. Biomol. Chem.*, 2015, **13**, 8298.
78. R. Cano, A. F. Schmidt and G. P. McGlacken, *Chem. Sci.*, 2015, DOI: 10.1039/C5SC01534K.
79. L. Djakovitch and F.-X. Felpin, *ChemCatChem*, 2014, **6**, 2175.
80. W. M. Alley, I. K. Hamdemir, K. A. Johnson and R. G. Finke, *J. Mol. Catal. A: Chem.*, 2010, **315**, 1.
81. E. Bayram, J. C. Linehan, J. L. Fulton, J. A. S. Roberts, N. K. Szymczak, T. D. Smurthwaite, S. Özkar, M. Balasubramanian and R. G. Finke, *J. Am. Chem. Soc.*, 2011, **133**, 18889.
82. M. Pagliaro, V. Pandarus, R. Ciriminna, F. Béland and P. Demma Carà, *ChemCatChem*, 2012, **4**, 432.
83. J. A. Widegren, M. A. Bennett and R. G. Finke, *J. Am. Chem. Soc.*, 2003, **125**, 10301.
84. F. Jafarpour, S. Rahiminejadan and H. Hazrati, *J. Org. Chem.*, 2010, **75**, 3109.
85. L. Djakovitch, V. Dufaud and R. Zaidi, *Adv. Synth. Catal.*, 2006, **348**, 715.
86. G. Cusati and L. Djakovitch, *Tetrahedron Lett.*, 2008, **49**, 2499.
87. N. Lrabasseur and I. Larrosa, *J. Am. Chem. Soc.*, 2008, **130**, 2926.
88. L. L. Chng, J. Zhang, J. Yang, M. Amoura and J. Y. Ying, *Adv. Synth. Catal.*, 2011, **353**, 2988.
89. J. Lee, J. Chung, S. M. Byun, B. M. Kim and C. Lee, *Tetrahedron*, 2013, **69**, 5660.
90. L. Zhang, P. Li, C. Liu, J. Yang, M. Wang and L. Wang, *Catal. Sci. Tech.*, 2014, **4**, 1979.
91. M. Al-Amin, M. Arisawa, S. Shuto, Y. Ano, M. Tobisu and N. Chatani, *Adv. Synth. Catal.*, 2014, **356**, 1631.
92. K. Takagi, M. Al-Amin, N. Hoshiya, J. Wouters, H. Sugimoto, Y. Shiro, H. Fukuda, S. Shuto and M. Arisawa, *J. Org. Chem.*, 2014, **79**, 6366.
93. S. Vásquez-Céspedes, A. Ferry, L. Candish and F. Glorius, *Angew. Chem. Int. Ed.*, 2015, **54**, 5772.
94. P. V. Reddy, M. Annapurna, P. Srinivas, P. R. Likhari and M. Lakshmi Kantam, *New J. Chem.*, 2015, **39**, 3399.
95. R. Kishore, J. Yadav, B. Venu, A. Venugopal and M. Lakshmi Kantam, *New J. Chem.*, 2015, **39**, 5259.
96. S. E. Bajwa, T. E. Storr, L. E. Hatcher, T. J. Williams, C. G. Baumann, A. C. Whitwood, D. R. Allan, S. J. Teat, P. R. Raithby and I. J. S. Fairlamb, *Chem. Sci.*, 2012, **3**, 1656.
97. K. J. Stowers, A. Kubota and M. S. Sanford, *Chem. Sci.*, 2012, **3**, 3192.
98. I. J. S. Fairlamb, *Angew. Chem. Int. Ed.*, 2015, DOI: 10.1002/anie.201411487, n/a.
99. Y. Sun, B. Mayers and Y. Xia, *Adv. Mater.*, 2003, **15**, 641.

## Journal Name

## ARTICLE

100. A. Dhakshinamoorthy, A. M. Asiri and H. Garcia, *Chem. Soc. Rev.*, 2015, **44**, 1922.
101. A. Dhakshinamoorthy and H. Garcia, *Chem. Soc. Rev.*, 2012, **41**, 5262.
102. Y. Huang, Z. Lin and R. Cao, *Chem. Eur. J.*, 2011, **17**, 12706.
103. Y. Huang, T. Ma, P. Huang, D. Wu, Z. Lin and R. Cao, *ChemCatChem*, 2013, **5**, 1877.
104. L. Wang, W.-b. Yi and C. Cai, *Chem. Commun.*, 2011, **47**, 806.
105. Y. M. A. Yamada, Y. Yuyama, T. Sato, S. Fujikawa and Y. Uozumi, *Angew. Chem. Int. Ed.*, 2014, **53**, 127.
106. T. Parsharamulu, D. Venkanna, M. Lakshmi Kantam, S. K. Bhargava and P. Srinivasu, *Ind. Eng. Chem. Res.*, 2014, **53**, 20075.
107. S. M. McAfee, J. S. J. McCahill, C. M. Macaulay, A. D. Hendsbee and G. C. Welch, *RSC Adv.*, 2015, **5**, 26097.
108. V. A. Zinovyeva, M. A. Vorotyntsev, I. Bezverkhyy, D. Chaumont and J.-C. Hierso, *Adv. Funct. Mater.*, 2011, **21**, 1064.
109. S. Keshipour and A. Shaabani, *Appl. Organomet. Chem.*, 2014, **28**, 116.
110. M. Shakeri, C.-w. Tai, E. Göthelid, S. Oscarsson and J.-E. Bäckvall, *Chem. Eur. J.*, 2011, **17**, 13269.
111. J. Malmgren, A. Nagendiran, C.-W. Tai, J.-E. Bäckvall and B. Olofsson, *Chem. Eur. J.*, 2014, **20**, 13531.
112. M. Cao, D. Wu, W. Su and R. Cao, *J. Catal.*, 2015, **321**, 62.
113. S. Korwar, K. Brinkley, A. R. Siamaki, B. F. Gupton and K. C. Ellis, *Org. Lett.*, 2015, **17**, 1782.
114. S. Wang, D. Hu, W. Hua, J. Gu, Q. Zhang, X. Jia and K. Xi, *RSC Adv.*, 2015, **5**, 53935.
115. D.-T. D. Tang, K. D. Collins and F. Glorius, *J. Am. Chem. Soc.*, 2013, **135**, 7450.
116. D.-T. D. Tang, K. D. Collins, J. B. Ernst and F. Glorius, *Angew. Chem. Int. Ed.*, 2014, **53**, 1809.
117. K. D. Collins, R. Honeker, S. Vasquez-Céspedes, D.-T. D. Tang and F. Glorius, *Chem. Sci.*, 2015, **6**, 1816.
118. R. Cano, A. F. Schmidt and G. P. McGlacken, *Chem. Sci.*, 2015, DOI: 10.1039/C5SC01534K.